#1

One-Dimensional Processing for Adaptive Image Restoration

Philip Chan

Technical Report 501

June 1984

Massachusetts Institute of Technology
Research Laboratory of Electronics
Cambridge, Massachusetts 02139

One-Dimensional Processing for Adaptive Image Restoration

Philip Chan

Technical Report 501

June 1984

Massachusetts Institute of Technology
Research Laboratory of Electronics
Cambridge, Massachusetts 02139

This work has been supported in part by the Advanced Research Projects Agency monitored by ONR under Contract N00014-81-K-0742 NR-049-506 and in part by the National Science Foundation under Grant ECS80-07102.

UNCLASSIFIED

SECURITY CLASSIFICATION OF THIS PAGE

REPORT DOCUMENTATION PAGE

1a. REPORT SECURITY CLASSIFICATION	1b. RESTRICTIVE MARKINGS
2a. SECURITY CLASSIFICATION AUTHORITY	3. DISTRIBUTION/AVAILABILITY OF REPORT Approved for public release; distribution unlimited
2b. DECLASSIFICATION/DOWNGRADING SCHEDULE	
4. PERFORMING ORGANIZATION REPORT NUMBER(S)	5. MONITORING ORGANIZATION REPORT NUMBER(S)
6a. NAME OF PERFORMING ORGANIZATION (6b. OFFICE SYMBOL (If applicable)) Research Laboratory of Electronics Massachusetts Institute of Technology	7a. NAME OF MONITORING ORGANIZATION Office of Naval Research Mathematical and Information Scien. Div.
6c. ADDRESS (City, State and ZIP Code) 77 Massachusetts Avenue Cambridge, MA 02139	7b. ADDRESS (City, State and ZIP Code) 800 North Quincy Street Arlington, Virginia 22217
8a. NAME OF FUNDING/SPONSORING ORGANIZATION (8b. OFFICE SYMBOL (If applicable)) Advanced Research Projects Agency	9. PROCUREMENT INSTRUMENT IDENTIFICATION NUMBER N00014-81-K-0742
8c. ADDRESS (City, State and ZIP Code) 1400 Wilson Boulevard Arlington, Virginia 22217	10. SOURCE OF FUNDING NOS. PROGRAM ELEMENT NO.: (unclassified) PROJECT NO.: TASK NO.: NR 049-506 WORK UNIT NO.:
11. TITLE (Include Security Classification) "One-Dimensional Processing for Adaptive Image Restoration"	
12. PERSONAL AUTHOR(S) Chan, Philip	
13a. TYPE OF REPORT: Technical 13b. TIME COVERED: FROM _____ TO _____	14. DATE OF REPORT (Yr., Mo., Day): 1984 June 15. PAGE COUNT: 100
16. SUPPLEMENTARY NOTATION Technical Report No. 501	
17. COSATI CODES: FIELD / GROUP / SUB. GR.	18. SUBJECT TERMS (Continue on reverse if necessary and identify by block number)

19. ABSTRACT (Continue on reverse if necessary and identify by block number)

A one-dimensional (1-D) approach to the problem of adaptive image restoration is presented. In this approach, we use a cascade of four 1-D adaptive filters oriented in the four major correlation directions of the image, with each filter treating the image as a 1-D signal. The objective of this 1-D approach is to improve the performance of the more general two-dimensional (2-D) approach. This differs considerably from previous 1-D approaches, the objectives of which have typically been to approximate a more general 2-D approach for computational reasons and not to improve its performance. The main advantage of this new 1-D approach is its capability to preserve edges in the image while removing noise in all regions of the image, including the edge regions. To illustrate this point, the approach is applied to existing 2-D image restoration algorithms. Experimental results with images degraded by additive white noise at various SNRs (signal-to-noise ratios) are presented. Further examples illustrate the application of 1-D restoration techniques based on this approach to images degraded by blurring and additive white noise and images degraded by multiplicative noise. Another example shows its usefulness in the reduction of quantization noise in pulse code modulation image coding.

20. DISTRIBUTION/AVAILABILITY OF ABSTRACT UNCLASSIFIED/UNLIMITED ☒ SAME AS RPT. ☐ OTIC USERS ☐	21. ABSTRACT SECURITY CLASSIFICATION Unclassified
22a. NAME OF RESPONSIBLE INDIVIDUAL Kyra M. Hall RLE Contract Reports	22b. TELEPHONE NUMBER (Include Area Code) (617) 253-2569 22c. OFFICE SYMBOL

DD FORM 1473, 83 APR EDITION OF 1 JAN 73 IS OBSOLETE.

UNCLASSIFIED

SECURITY CLASSIFICATION OF THIS PAGE

ONE-DIMENSIONAL PROCESSING FOR ADAPTIVE IMAGE RESTORATION

by Philip Chan

Submitted to the Department of Electrical Engineering and Computer Science, on May 11, 1984, in partial fulfillment of the requirements for the degree of Master of Science in Electrical Engineering and Computer Science.

ABSTRACT

A one-dimensional (1-D) approach to the problem of adaptive image restoration is presented. In this approach, we use a cascade of four 1-D adaptive filters oriented in the four major correlation directions of the image, with each filter treating the image as a 1-D signal. The objective of this 1-D approach is to improve the performance of the more general two-dimensional (2-D) approach. This differs considerably from previous 1-D approaches, the objectives of which have typically been to approximate a more general 2-D approach for computational reasons and not to improve its performance. The main advantage of this new 1-D approach is its capability to preserve edges in the image while removing noise in all regions of the image, including the edge regions. To illustrate this point, the approach is applied to existing 2-D image restoration algorithms. Experimental results with images degraded by additive white noise at various SNRs (signal to noise ratios) are presented. Further examples illustrate the application of 1-D restoration techniques based on this approach to images degraded by blurring and additive white noise and images degraded by multiplicative noise. Another example shows its usefulness in the reduction of quantization noise in pulse code modulation image coding.

Thesis Supervisor: Professor Jae S. Lim

Title: Associate Professor of Electrical Engineering

ACKNOWLEDGEMENTS

My deepest appreciation goes to Professor Jae S. Lim for his supervision of this thesis. His encouragement, understanding, and patience have made my graduate study at MIT a very fruitful and enjoyable one.

I would like to thank all members of the Digital Signal Processing Group at MIT who provided an excellent research environment. Special thank goes to members of the Cognitive Information Processing Group at MIT who assisted me in producing hard copies of the images in this thesis on their facilities.

I am deeply indebted to my parents whose care and teaching have played an important role in the success of my study.

Special thanks are due to my wife, Ai Hwa. Her loving care and encouragement have supported me throughout my stay at MIT. She has also helped in the preparation of this document.

Finally, I gratefully acknowledge the financial support by the Government of Singapore whose DSO Scholarship has supported my graduate education.

TABLE OF CONTENTS

LIST OF FIGURES

LIST OF TABLES

CHAPTER 1

INTRODUCTION

1.1 Introduction

Image restoration is the reconstruction of a degraded image towards the original object by the reduction or removal of the degradations. These degradations may be introduced during the formation, transmission and reception of the image. For example, an out-of-focus camera, or the relative motion between the camera and the object, blurs the recorded picture; an image sensor circuit or a transmission channel may introduce random noise to the picture; an aerial photograph may suffer from distortion due to air turbulence. Because of the recent advances in computer technology, digital image restoration has received considerable attention for a large number of applications, such as astronomy, remote sensing, medical imagery, and aerial reconnaissance.

In this thesis, the primary concern is the reduction of noise in the observed image. The noise reduction system is useful for images which suffer from little or no blurring. It is also useful for a class of restoration techniques where the blurred and noisy image is processed by a noise reduction system prior to the deblurring process. Sufficient noise reduction would improve the performance of the deblurring process.

The performance of an image restoration system depends on the accuracy of the model adopted for the image. Better performance can be expected if a more accurate model is used. However, to accurately model an image is a difficult task, because an image is generally neither periodic nor stationary, and

its formation cannot be characterized by a simple parametric model. As a result, a model that accurately describes an image is likely to be very complex. Even if an accurate model could be found, difficulties could arise in the estimation of the model parameters and implementation of the restoration system. Due to these difficulties, a compromise is often made between a simpler model and the performance of the restoration system.

In designing an image restoration system, we must also consider the criterion that is used to judge the performance of the system. In many applications, the restored images are to be viewed by human observers. Therefore, the image restoration system should be compatible with the human visual system in some optimum way. This is, however, a difficult task, because of the limited understanding of the complex human vision system. Although one may define a measurable objective criterion such as the minimization of the mean square error between the original and processed images, it should not be taken as an absolute criterion. For example, a blurred picture may have a small mean square error, but it may not be acceptable to human viewers. On ther other hand, a more subjective criterion, such as the preservation of details in the picture, may be more suitable for the human viewers. However, such a criterion may not be easily incorporated in the optimization process.

Numerous mathematically optimal image restoration techniques have been proposed [1,2]. The earlier techniques are mostly linear methods, due to their simplicity in analysis and computations. Based on the assumption that the signal and noise processes are statistically stationary, these linear methods result in space invariant filters designed by using some average characteristics of the signal. Specifically, for a noise reduction system, these filters are some

form of a low pass filter which removes noise components at high spatial frequencies. Unfortunately, low pass filters also suppress the high frequency components of the image, which convey important information about the edges and fine details of the objects in the image. The result is an undesirable blurring of the image.

The stationarity assumption used in these linear techniques is generally invalid in real images. For example, the correlation between adjacent picture elements (pixels) in one part of a picture with a lot of spatial activities is significantly different from the correlation in another part which is relatively flat. A low pass filter, based on the signal characteristics in the flat areas, will perform well in the flat areas but will blur the details in the edge areas.

Many adaptive systems have been proposed to overcome this difficulty. In these systems, a nonstationary model is assumed, and the model parameters are updated with the changes in image properties. The restoration filter is then adapted to the varying model parameters. In general, adaptation could be made continuously from pixel to pixel. However, this would require a large amount of computations. In order to reduce computations, the adaptation model has to be kept simple. An alternative approach is to partition the image into regions or subimages. Within each region or subimage, a locally stationary model is assumed, and a filter is designed with the parameters estimated for that region. Although adaptive systems are computationally more expensive in both design and implementation, they perform significantly better than non-adaptive methods.

Images are two-dimensional (2-D) signals. Consequently, most image restoration systems are 2-D processes. Images may also be treated as one-

dimensional (1-D) signals, so that 1-D signal processing techniques may be applied. A simple way to characterize an image is to consider it as a collection of 1-D signals, e.g., the output of a raster scanner [3], or a sequence of rows or columns [4]. 1-D stochastic models can then be applied, and result in 1-D restoration of the scanner output or the individual rows or columns. This has a disadvantage in that some image correlation information is lost in the conversion from the 2-D domain to the 1-D domain.

1-D filters are sometimes used to approximate a 2-D filter. In an adaptive image restoration system, a 2-D filter is generally obtained at each pixel or subimage, using the local image characteristics in the surrounding region. Since the filter has to be determined at every pixel or subimage, adaptive systems are computationally expensive. In order to reduce computation, the 2-D filter is sometimes designed or implemented by several 1-D filters as an approximation to the 2-D filter. This approach generally gives suboptimal performance compared with the original 2-D filter.

1.2 Scope of the Thesis

Many adaptive image restoration systems apply a 2-D spatially variant filter to the degraded image. The filter is typically determined from a small local region of the image based on some simple mathematical criterion such as the mean square error minimization. Within the local region, the image is usually assumed to be a sample of a stationary random process so that methods, such as Wiener filtering, can be used to determine the filter coefficients. A major problem of this approach often occurs in edge regions where the signal

cannot be adequately modeled, even locally, as a sample of a stationary random process, and a filter determined with this assumption may not be able to both preserve edges and reduce noise at the same time.

In this thesis, a new 1-D approach to adaptive image restoration is proposed which aims to achieve better noise reduction near edges while preserving the edges. The objective of this approach is to improve the performance of the more general 2-D approach. This differs considerably from previous 1-D approaches, the objectives of which have typically been to approximate a more general 2-D approach for computational reasons and not to improve its performance. More specifically, restoration systems developed based on this 1-D approach remove noise more effectively than their 2-D counterparts, without compromising the resolution of the image.

In this approach, four 1-D adaptive filters oriented in the four major correlation directions of the image are applied sequentially to the image. Each of the four filters is designed based on the same image model and basic principle used in the development of a 2-D adaptive image restoration system. Thus, the noise at an edge is removed by one of the 1-D filters oriented approximately in the same direction as the edge. Since each filter is adaptive and edge preserving, sequential application of the four filters does not blur the edge.

The usefulness and limitation of this approach will be studied by application to existing 2-D image restoration methods for images degraded by additive white noise. Although the approach is developed primarily for the reduction of noise in images, its performance in a noise-reduction-deblurring restoration system will be studied. Other examples that are studied as a part of this thesis are: a) images degraded by multiplicative noise, and b) quantization noise

reduction in a low bit rate image coding system.

In summary, this thesis proposes a new 1-D approach to adaptive image restoration, discusses its implementation and evaluates its performance.

1.3 Organization of Chapters

This thesis is organized in six chapters.

In Chapter 2, examples of the common image restoration techniques are reviewed to illustrate the general principle as well as the limitations of nonadaptive and adaptive approaches to image restoration. Some restoration systems using 1-D approximations to 2-D restoration will also be studied.

Based on the discussion in Chapter 2, a new 1-D image restoration approach is developed in Chapter 3 for images degraded by additive noise. The motivation and practical aspects of the approach are discussed.

In Chapter 4, the 1-D approach developed in Chapter 3 is applied to three existing 2-D adaptive systems to illustrate its usefulness and limitations. The first system is a simple algorithm based on local statistics of the image [5]. In the original 2-D method, edges are modeled by higher signal variances, while the orientation of the edge is not taken into account in the model. This results in insufficient noise removal near edges. Using the new 1-D approach, the modified system improves the performance by reducing the noise near edges. In the second example, an adaptive filter is designed based on the lower sensitivity of the human visual system to noise near edges [6]. Similar improvement to this filter can be achieved with the new 1-D approach. The third system is a short

space spectral subtraction technique implemented in the frequency domain [7]. In the 2-D method, the spectrum of the original image is estimated by subtracting the noise spectrum from the observed image spectrum. The 1-D implementation of the technique illustrates a limitation of the 1-D approach.

In Chapter 5, three further applications of the 1-D approach are shown. The first application is the restoration of images degraded by blurring as well as additive noise. Following an approach in [7], the degraded image is processed by a 1-D noise reduction technique developed in Chapter 4, before it is deblurred by inverse filtering. The noise reduction avoids the instability problem often associated with inverse filtering. The second application demonstrates the effectiveness of the 1-D technique in the density (log intensity) domain to restore images corrupted by multiplicative noise. In the third application, the 1-D method is used as a post-processor for a particular bit rate reduction scheme known as the Roberts' pseudonoise method [9]. In this scheme, the signal-dependent quantization noise associated with low bit rate quantization is converted to less objectionable signal-independent random noise. The 1-D method improves the appearance of the image by reducing the amount of random noise.

In the final chapter, a summary of results is given along with suggestions for future research using the 1-D approach.

CHAPTER 2

REVIEW OF IMAGE RESTORATION

2.1 Introduction

Numerous methods have been proposed to solve the problem of image restoration. Some are ad-hoc; others are solutions to some optimization problems. There are various ways to categorize these techniques, according to the assumptions made about the image, the restoration criterion, and their implementation. For the purpose of this thesis, they will be classified as either nonadaptive or adaptive. The major difference between these two categories lies in the assumptions made about the image model: a stationary model generally leads to nonadaptive techniques, and a nonstationary model leads to adaptive techniques.

Some examples of both nonadaptive and adaptive image restoration will be reviewed to illustrate the general assumptions, principles and limitations of the two approaches. Although adaptive processing generally performs better than nonadaptive processing, it incurs heavy computational loads. Sometimes, the computational loads may be reduced by using 1-D approximations to the 2-D adaptive approach. The general principle of these approximations will be studied.

2.2 Representations of Images and Degradations

Depending upon the specific application and processing technique employed, an image may be represented in several different ways, e.g., space domain versus frequency domain representation; 2-D versus 1-D representation. In this section, the various representations will be discussed, followed by a description of the commonly used image and degradation models.

Image Representation

Let $g(x,y)$ be a continuous image in the image plane (x,y). To represent the image in the discrete form for digital processing, it is necessary to sample the continuous image according to the two-dimensional sampling theorem. Thus, if the Nyquist criterion is satisfied, the image may be represented by the 2-D sequence $g(n_1,n_2)$ where n_1 and n_2 are, respectively, the distance indices in the horizontal and vertical directions.

Another discrete representation of the image is obtained by raster scanning the image to form a 1-D vector g, where

$$\mathbf{g} = \begin{bmatrix} g(1,1) \\ g(1,2) \\ \vdots \\ g(1,N) \\ g(2,1) \\ \vdots \\ g(N,N) \end{bmatrix} \tag{2.1}$$

where $N \times N$ is the size of $g(n_1,n_2)$. This representation is most useful in linear algebraic restoration methods.

In the frequency domain, $g(n_1,n_2)$ is represented by its Fourier transform defined as

$$G(\omega_1,\omega_2) = \sum_{n_1=0}^{N-1} \sum_{n_2=0}^{N-1} g(n_1,n_2)\, e^{-j\omega_1 n_1}\, e^{-j\omega_2 n_2} \tag{2.2}$$

This representation is useful for processing in the frequency domain.

One useful representation often used in recursive algorithms is that of state space representation. It may take many different forms depending on the state variables chosen. In state space representation, the image is modeled as the output of a dynamical system, which relates the present state at a pixel of the image to the states of its neighbors. A general form of the dynamical model is given by

$$\mathbf{s}(n) = \mathbf{A}(n)\mathbf{s}(n-1) + \mathbf{B}(n)\mathbf{u}(n) \tag{2.3}$$

$$\mathbf{r}(n) = \mathbf{C}(n)\mathbf{s}(n) + \mathbf{w}(n) \tag{2.4}$$

where **s** is the state vector, **r** is the observation, **w** is the observation noise, and **u** is the white noise that drives the system. **A**, **B** and **C** are, respectively, the system, drive and observation matrices. State space representation is typically used in the causal estimation of a future pixel from the noisy observation and some amount of information about past and present estimates.

Image Formation

To restore images suffering from spatial degradation, such as blurring, the degradation must be characterized mathematically. Let $g(n_1,n_2)$ be an image of an object $f(k_1,k_2)$. In practical imaging systems, the intensity of the image at the point (n_1,n_2), $g(n_1,n_2)$, is a function of $f(k_1,k_2)$. If the function is

linear, the general description of g is

$$g(n_1,n_2) = \sum_{k_1} \sum_{k_2} h(n_1,n_2;k_1,k_2)\, f(k_1,k_2) \tag{2.5}$$

The function h is referred to as the point spread function (PSF). If h is assumed space invariant,

$$g(n_1,n_2) = \sum_{k_1} \sum_{k_2} h(n_1-k_1,n_2-k_2)\, f(k_1,k_2)$$

$$= h(n_1,n_2) * f(n_1,n_2) \tag{2.6}$$

where * denotes 2-D convolution. In terms of vector-matrix representation,

$$\mathbf{g} = \mathbf{H}\mathbf{f} \tag{2.7}$$

where **g** and **f** are vector created in the manner described by Eqn. (2.1), and **H** is a $N^2 \times N^2$ matrix created from $h(n_1,n_2)$.

In the frequency domain, Eqn. (2.6) can be written, by taking Fourier Transforms on both sides, as

$$G(\omega_1,\omega_2) = H(\omega_1,\omega_2) F(\omega_1,\omega_2) \tag{2.8}$$

where $G(\omega_1,\omega_2)$, $F(\omega_1,\omega_2)$ and $H(\omega_1,\omega_2)$ are the Fourier transforms of $g(n_1,n_2)$, $f(n_1,n_2)$, and $h(n_1,n_2)$ respectively.

Point Spread Function

The PSF $h(n_1,n_2;k_1,k_2)$ is the response of the imaging system to a unit point source located at (k_1,k_2). It can be used to characterize many distortion and blurring effects of the imaging system. One such example is the long term exposure in atmospheric turbulence, where the PSF is approximately Gaussian

and given by

$$H(\omega_1,\omega_2) = e^{-\frac{1}{2}\frac{\omega_1^2+\omega_2^2}{\sigma^2}} \tag{2.9}$$

where σ^2 determines the degree of spreading.

Image Model

An image is described by a model which is an abstraction of the structure of the image or of a class of images. One commonly used model in image restoration is a statistical model. An image is then a sample of the random process described by the model.

If the probability density function (PDF) of the image process is known, the parameters of the PDF completely describe the image. One example is the multivariate Gaussian PDF, which is fully characterized by its mean vector $\bar{f}$ and covariance matrix Φ_f defined, respectively, by

$$\bar{f} = E[f] \tag{2.10}$$

and

$$\Phi_f = E[(f-\bar{f})(f-\bar{f})^T] \tag{2.11}$$

where $E[\cdot]$ denotes expectation. In most cases, the specific PDF is not known. A good, concise description of the image can still be given by the mean $\bar{f}$ and the covariance function Φ_f.

A common assumption on image model is that of stationarity. A random process is said to be strict-sense stationary (SSS) if the joint PDF of any collection of samples depends only upon the spacing between samples. Because it is usually difficult to show that a given process is SSS, a more practical and

more common assumption of stationarity is that of wide-sense stationarity. An image is wide-sense stationary if the mean is constant and the correlation between pixels is independent of the absolute locations of the pixels, i.e.,

$$\bar{f}(n_1,n_2) = E[f(n_1,n_2)] = constant \tag{2.12}$$

$$R(n_1,n_2;k_1,k_2) = E[f(n_1,n_2)f(k_1,k_2)] = R(n_1-k_1,n_2-k_2) \tag{2.13}$$

In this case, Φ_f as defined in Eqn. (2.11) has a block Toeplitz structure.

Noise Model

A noise model commonly assumed in image restoration is that of additive white noise. A degraded noisy image may then be described by

$$g(n_1,n_2) = f(n_1,n_2) * h(n_1,n_2) + w(n_1,n_2) \tag{2.14}$$

where $w(n_1,n_2)$ is a signal-independent white noise sequence. Many physical noise processes can be approximated as white noise, e.g., random thermal noise in image sensor circuits.

Another common noise model is that of multiplicative noise. It is described by

$$g(n_1,n_2) = [f(n_1,n_2) * h(n_1,n_2)]w(n_1,n_2) \tag{2.15}$$

One example of multiplicative noise is the speckle noise in laser generated images. In general, if an additive noise component is proportional to the signal, it can also be modeled as multiplicative noise.

2.3 Nonadaptive Image Restoration

In a stationary image model, an image is assumed to be a sample of a wide-sense stationary random process with a constant mean vector and a block Toeplitz covariance matrix. Linear filtering, generally based on some least square criteria, can then be applied to obtain an estimate of the original image from the degraded observed image. The filter may be implemented in the frequency domain to take advantage of the computational efficiency of the FFT (Fast Fourier Transform) algorithm. In the space domain, using state space representation and a causal model, recursive algorithms also result in efficient implementation. Two typical examples of linear filtering will be discussed.

Wiener Filter

The following model is assumed:

$$\mathbf{g} = \mathbf{H}\mathbf{f} + \mathbf{w} \tag{2.16}$$

where $\mathbf{f}$ is assumed zero-mean and $\mathbf{w}$ is signal independent. It is also assumed that the image correlation and the noise process are known *a priori*. By imposing a minimum-mean-square-error criterion, which minimizes the expected error $\mathbf{f}-\hat{\mathbf{f}}$ of the estimate $\hat{\mathbf{f}}$ over the ensemble of all possible images, i.e.,

$$\min_{\hat{\mathbf{f}}} E\left[(\mathbf{f}-\hat{\mathbf{f}})^T(\mathbf{f}-\hat{\mathbf{f}})\right] \tag{2.17}$$

the estimate was derived by Helstrom [11] as

$$\hat{\mathbf{f}} = \Phi_f H^T (H \Phi_f H^T + \Phi_w)^{-1}\mathbf{g} \tag{2.18}$$

where Φ_f and Φ_w are the autocovariance matrices of $\mathbf{f}$ and $\mathbf{w}$ respectively

Because of the high dimensionality of the matrices ($N^2 \times N^2$), Eqn. (2.18) cannot be evaluated efficiently. However, if f and w are stationary processes, then Φ_f and Φ_w are block Toeplitz, and Eqn. (2.18) can be evaluated by DFT (Discrete Fourier Transform) approximation as

$$\hat{F}(k_1,k_2) = \frac{H^*(k_1,k_2)}{|H(k_1,k_2)|^2 + \dfrac{P_w(k_1,k_2)}{p_f(k_1,k_2)}} G(k_1,k_2) \tag{2.19}$$

where $F(k_1,k_2)$, $G(k_1,k_2)$, and $H(k_1,k_2)$ are the DFT's of $f(n_1,n_2)$, $g(n_1,n_2)$, and $h(n_1,n_2)$ respectively. $P_f(k_1,k_2)$ and $P_w(k_1,k_2)$ are the discrete samples of the *a priori* power spectra of $f(n_1,n_2)$ and $w(n_1,n_2)$ respectively. Thus, if $H(k_1,k_2)$ is also known *a priori*, $\hat{f}(n_1,n_2)$ may be obtained by the inverse DFT of $\hat{F}(k_1,k_2)$ calculated from Eqn. (2.19).

2-D Kalman filter

The application of recursive methods in image restoration is motivated by the success of Kalman filtering in 1-D filtering and prediction problems. With the techniques of spectral factorization, the dynamic model of the image random field may be described by a partial difference equation that is recursively computable. The direct extension of the Kalman filter to image restoration was first studied by Habibi [12]. In his approach, Habibi assumed that the random field is a separable 2-D first order Markov process whose autocorrelation function is given by

$$R(k_1,k_2) = \sigma_f^2 e^{-\alpha_1|k_1|} e^{-\alpha_2|k_2|} \tag{2.20}$$

The image can then be represented as the output of the following autoregressive system

$$f(n_1+1,n_2+1) = \rho_1 f(n_1+1,n_2) + \rho_2 f(n_1,n_2+1) - \rho_1\rho_2 f(n_1,n_2)$$

$$+ \sqrt{(1-\rho_1^2)(1-\rho_2^2)}\, u(n_1,n_2) \qquad (2.21)$$

where the correlation coefficients ρ_1, ρ_2 are given respectively by

$$\rho_1 = e^{-\alpha_1} \qquad (2.22)$$

and

$$\rho_2 = e^{-\alpha_2} \qquad (2.23)$$

and $u(n_1,n_2)$ is a white noise sequence.

The minimum mean square error estimate of f is given recursively by

$$\hat{f}(n_1+1,n_2+1) = \rho_1 \hat{f}(n_1+1,n_2) + \rho_2 \hat{f}(n_1,n_2+1)$$

$$+[\rho_1\rho_2 + K(n_1,n_2)]\hat{f}(n_1,n_2) + K(n_1,n_2)y(n_1,n_2) \qquad (2.24)$$

where $K(n_1,n_2)$, a spatially varying function of g, is also recursively computable. Thus, if α_1 and α_2 are known, Eqn. (2.24) recursively generates all values of $\hat{f}$, given assumed boundary conditions at the topmost row and leftmost column of the image.

Discussion

In these examples, as well as in their other extensions, the autocorrelation function of the original image (or equivalently, its power spectrum) must be known *a priori*. This is not true in most practical situations. The autocorrelation function can also be estimated by some other means, for example, by averaging the autocorrelation functions of several prototype images. However, the accuracy of this approach is questionable. These techniques also require that the image be stationary to achieve efficient algorithms. In the Wiener

filter, for example, nonstationary correlation matrices make fast implementation in the frequency domain impossible. In the 2-D Kalman filter, although nonstationarity may be accounted for by spatially varying correlation functions, estimating them in the noisy image remains a difficult task.

Pictures processed by nonadaptive techniques generally appear to be too smooth. This is partly because the solutions are obtained by a minimum mean square error criterion, which is not the criterion the human visual system uses to judge the quality of an image. More importantly, the smoothness is caused by the simple stationary assumption which is invalid in most images.

2.4 Adaptive Image Restoration

The previous section illustrated the shortcomings of nonadaptive linear restoration procedures. The main difficulty was due to the assumption of stationarity. The general approach to solving this problem is to perform subimage processing, in which the image is first divided into subimages. Each subimage is then processed independently, assuming local stationarity. In this case, the model parameters have to be determined for every subimage. In order to reduce the amount of calculation, the model is often a simple one, as illustrated by the two following examples. The first example deals with nonlinear sensor characteristics. The second example is an adaptive Kalman filter.

Sectioned MAP method

Trussell and Hunt [13] derived a maximum *a posteriori* (MAP) method for restoring images degraded by nonlinear sensor characteristics, as described

by

$$\mathbf{g} = s[\mathbf{Hf}] + \mathbf{w} \tag{2.25}$$

where $s[\cdot]$ represents the nonlinearity. Using the multivariate Gaussian assumption for **f** and **w**, the solution is given by an implicit equation :

$$\hat{\mathbf{f}} = \bar{\mathbf{f}} + \Phi_f \mathbf{H}^T \mathbf{S}_b \Phi_w^{-1}\left[\mathbf{g} - s[\mathbf{H}\hat{\mathbf{f}}]\right] \tag{2.26}$$

where $\bar{\mathbf{f}}$ is the *a priori* mean of the original image and $\mathbf{S}_b$ is a diagonal matrix of derivatives of s.

By dividing the image into blocks, Eqn. (2.26) is solved iteratively for the estimate in each block. To simplify the computation, Φ_f and Φ_w are replaced by σ_f^2 and σ_w^2 respectively, i.e., the spatial correlation is ignored. The estimate for block m is, therefore,

$$\hat{\mathbf{f}}_m = \bar{\mathbf{f}}_m + \frac{\sigma_f^2}{\sigma_w^2}\mathbf{H}^T \mathbf{S}_b \left[\mathbf{g}_m - s[\mathbf{H}\hat{\mathbf{f}}_m]\right] \tag{2.27}$$

The results are combined by the overlap save method.

Adaptive Kalman Filter

Instead of dividing the image into fixed-sized blocks, the partitioning can also be done by other means. For example, the image can be partitioned into regions according to local correlation characteristics. Then, a filter using the correlation parameters in each region can be implemented. In [14], partitioning is done by thresholding the spatial activities at each pixel, measured in terms of signal directional slope information, into one of M values. Each region is then characterized by one of M stationary autocorrelation functions which, for simplicity, are assumed to be exponential and separable. The

correlation coefficients ρ_1, ρ_2 are determined for each of the autocorrelation functions. A bank of Kalman filters are then run in parallel, one for each region, with special care to the boundary conditions at the border between regions.

Discussion

In most adaptive restoration systems, the algorithm implemented in a local region is generally a straightforward extension of the global nonadaptive algorithm. Since local signal characteristics must be determined for each subimage or region, the image model for each subimage or region has to be kept simple to reduce the amount of computation in both model parameter identification and filter implementation.

Partitioning of the image may be done block by block or by variable size and shape. Since each subimage is processed by a filter which may be significantly different from the ones in the adjacent subimages, care must be taken in combining the results of neighboring subimages, as well as in matching boundary conditions at the border.

2.5 One-Dimensional Approximations to Two-Dimensional Image Restoration

In this section, we will summarize some restoration techniques using 1-D processing. Such 1-D processing is typically used as an approximation to the 2-D approach, partly because of the difficulty in establishing a good 2-D image model, and partly to reduce the heavy computational loads associated with adaptive filtering.

Restoration Based on a Multiple Fragment Model

In [15], Lebedev and Mirkin assumed that an image is composed of five classes of fragments. Each class of fragments is distinguished by the type of correlational links between the elements and characterized by a specific correlation R_θ $(1 \le \theta \le 5)$. Four of the classes correspond to prominent correlational links in the four directions at 0°, 45°, 90° and 135°. The fifth describes fragments with an isotropic structure. It is assumed that $p(\theta)$, the *a priori* probability density of the five classes, is known. For each class θ, $p(g \mid \theta)$, the conditional probability density of the image data, is assumed Gaussian and known.

The estimate of f in a window is calculated as follows. Let $\hat{f}(n_1,n_2 \mid \theta)$ be the conditional estimate of f assuming that the windowed data belong to the particular fragment class θ. For each θ, since R_θ is assumed known, $\hat{f}(n_1,n_2 \mid \theta)$ can be calculated by linear methods, for example, Wiener filter. Let $p(\theta \mid g)$ be the *a posteriori* probability that the windowed data belong to the class θ. $p(\theta \mid g)$ can be obtained by Bayes rule as

$$p(\theta \mid g) = \frac{p(\theta)\, p(g \mid \theta)}{\sum_{\theta=1}^{5} p(\theta)\, p(g \mid \theta)} \tag{2.28}$$

The estimate of f is then the sum of the conditional estimate $\hat{f}(n_1,n_2 \mid \theta)$, weighted by $p(\theta \mid g)$, i.e.,

$$\hat{f}(n_1,n_2) = \sum_{\theta=1}^{5} p(\theta \mid g)\, \hat{f}(n_1,n_2 \mid \theta) \tag{2.29}$$

In summary, the image data in a moving window are filtered by four 1-D filters and a 2-D averaging filter. The restored image is given by the sum of the five outputs with weights equal to $p(\theta \mid g)$.

Modified Wiener Filter

Abramatic and Silverman [16] derived two spatially variant filters for restoring unblurred but noisy images. The filters are Wiener filters modified by a visibility function $F(n_1,n_2)$ proposed by Anderson and Netravali [6]. The transfer functions of the two filters are

$$H_R(\omega_1,\omega_2;n_1,n_2) = \frac{P_f(\omega_1,\omega_2;n_1,n_2)}{P_f(\omega_1,\omega_2;n_1,n_2) + F(n_1,n_2)\sigma_w^2} \tag{2.30}$$

and

$$H_R(\omega_1,\omega_2;n_1,n_2) = F(n_1,n_2)\frac{P_f(\omega_1,\omega_2;n_1,n_2)}{P_f(\omega_1,\omega_2;n_1,n_2) + \sigma_w^2} + [1-F(n_1,n_2)] \tag{2.31}$$

where $P_f(\omega_1,\omega_2;n_1,n_2)$ is the local power spectrum of f at (n_1,n_2). The noise is assumed additive and white with power σ_w^2.

The sequence $F(n_1,n_2)$, with values between 0 and 1, is a monotonically decreasing function of the 'busyness' of the pixel at (n_1,n_2). As $F(n_1,n_2)$ varies from 0 to 1, the filters are a compromise between the identity filter and the Wiener filter. Thus, in edge regions where $F(n_1,n_2)$ is close to 0, the filters approach the identity filter, and edges are preserved.

Since $P_f(\omega_1,\omega_2;n_1,n_2)$ has to be estimated at every point (n_1,n_2), two suboptimal procedures were proposed. In both procedures, the image is described by a single known power spectrum. Its nonstationary properties are contained only in the space varying visibility function $F(n_1,n_2)$. In the first procedure, both the power spectrum and the restoration filters are assumed separable so that $H_R(\omega_1,\omega_2;n_1,n_2)$ can be approximated by a horizontal filter $H_1(\omega_1;n_1,n_2)$ and a vertical filter $H_2(\omega_2;n_1,n_2)$. In the second procedure, a 1-D

filter calculated by either Eqn. (2.30) or Eqn. (2.31) is determined for each of the 4 directions at 0°, 45°, 90°, and 135°. The approximate 2-D filter is reconstructed by bilinearly interpolating the four filters.

Order Constrained Median Filter

In [17], the estimate at a pixel is given by the average of the outputs of two 1-D filters oriented in the horizontal and vertical directions. Within each filter window, the filtering process consists of two steps. The first step is a trend detection scheme based on a simple hypothesis test. Assuming that the *a priori* means of the image data in the window are $m_1, m_2, \cdots, m_n$, the trend of the data, assumed to be either monotonically increasing or monotonically decreasing, is determined by the hypothesis test:

$$H_0 : m_1 \leq m_2 \leq \cdots \leq m_n \tag{2.32}$$

versus

$$H_1 : m_1 \geq m_2 \geq \cdots \geq m_n \tag{2.33}$$

Under each hypothesis, the maximum likelihood estimate of m_i, constrained by the assumed trend of the data, is determined. In step two, the median of the estimate $\hat{m}_i$, obtained under the selected hypothesis, is taken as the output of the 1-D filter.

Discussion

Approximations to 2-D restoration filter arise from the difficulty in obtaining the local edge information or the local power spectrum from the degraded image. As illustrated by the examples, one way to approximate a 2-D filter is to assume that the filter is separable. This leads to cascaded 1-D filters

in the horizontal and vertical directions. A more common approach is to sum, average, or select the outputs of several 1-D filters running in parallel. These approximations generally give suboptimal performance compared to the truly 2-D approach, although the amount of computation is reduced.

2.6 Summary

This chapter reviewed the common approaches to image restoration. The earlier approach based on linear filtering is not suited to the nonstationary nature of practical images. Adaptive restoration by subimage processing has been the general approach adopted recently. One disadvantage of such an approach is the amount of computation required. Primarily to reduce computation, several 1-D processing schemes have been proposed as an approximation to the 2-D adaptive filter. However, such an approximation would result in suboptimal performance. In the next chapter, a new 1-D approach to adaptive image restoration will be presented.

CHAPTER 3

A ONE-DIMENSIONAL APPROACH TO ADAPTIVE IMAGE RESTORATION

3.1 Introduction

From the brief review in chapter 2, one can conclude that a good image restoration system

(1) should be based on a nonstationary image model and able to adapt to the changing characteristics of an image,

(2) should require little *a priori* information about the original image and estimate the filter parameters from the observed image,

(3) should be easy to implement and require minimal computational efforts, and

(4) should reduce noise while preserving edges and details in the image.

Many existing restoration methods possess these properties, but their performance has rooms for improvement. More specifically, some of these methods are based on simple nonstationary image models, and preserve edges by removing less noise in the edge areas than in the flat areas. As a result, the edge areas appear noisy, especially for images at low signal to noise ratios (SNR). In this chapter, a new approach making use of 1-D filters is proposed. The objective of this approach is to improve the performance of the general 2-D approach for some adaptive image restoration systems.

3.2 Motivation of the Approach

Ideally, the desired filter that would remove noise in all regions, including the edge regions, should have a large support in flat areas for better noise smoothing. In the edge regions, the filter should be nonisotropic and change its shape and size to adapt to the edges in order to reduce noise at the edges and to preserve the edges.

Examination of some adaptive restoration techniques [e.g., 5,6] reveals that the filters are

(1) based on a simple image model which is insensitive to the orientation of the edges,

(2) of the same support size regardless of the image characteristics, and

(3) isotropic, i.e., symmetrical in all directions about the original.

As a consequence, the performance of these filters is not satisfactory.

One approach to achieve better noise reduction and edge preservation is to model the image more accurately (considering an image edge as a deterministic component, for example) and develop a new image restoration algorithm based on the new model. However, modeling an image accurately is a difficult task, and the resulting image restoration algorithm based on a detailed accurate image model is likely to be quite complex.

A much simpler approach is to use a 1-D filter without changing the image model or the basic principle used in developing a 2-D image restoration system. If a 1-D filter is allowed to change its orientation, it may be aligned in the same direction as the edge, and avoid intersecting the edge. In this manner,

the noise at the edge is removed and the edge is preserved. The next section presents a 1-D approach to image restoration which is simple, does not require an explicit edge detector to orient a 1-D filter, and can be applied to both edge and non-edge regions. As will be discussed in the next chapter, when the 1-D approach is applied to some existing 2-D image restoration algorithms, techniques developed based on the 1-D approach performs significantly better than the corresponding 2-D techniques.

3.3 The Basic Principle

Consider an image $f(n_1,n_2)$ degraded by some noise $w(n_1,n_2)$. The degraded image will be denoted by $g(n_1,n_2)$. If a 2-D adaptive filter is represented as $T[\cdot]$, $\hat{f}(n_1,n_2)$, the output of the adaptive filter, can be represented as

$$\hat{f}(n_1,n_2) = T[g(n_1,n_2)] \tag{3.1}$$

The adaptive filter $T[\cdot]$ is typically determined from a local 2-D region (or window) of the image surrounding (n_1,n_2) based on some image restoration principle, such as Wiener filtering.

Let $T_i[\cdot]$, $(1 \le i \le N)$, represent the 1-D filter, which is obtained in the same way as the 2-D adaptive filter, but determined from a local 1-D region (or window) oriented in the i^{th} direction. For practical reasons, let $N=4$, and let the four directions be the major correlation directions of most practical images, i.e., 0, 90, 45 and 135 degrees. The noisy image is filtered by a cascade of the four filters, as if the image were a 1-D signal for each of the filters (Figure 3.1).

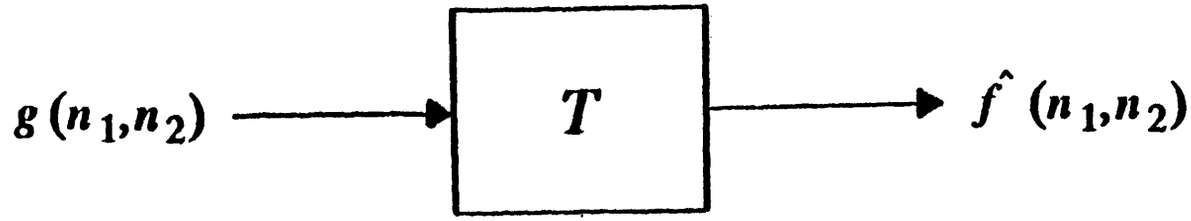

Figure 3.1 (a) A 2-D restoration method.

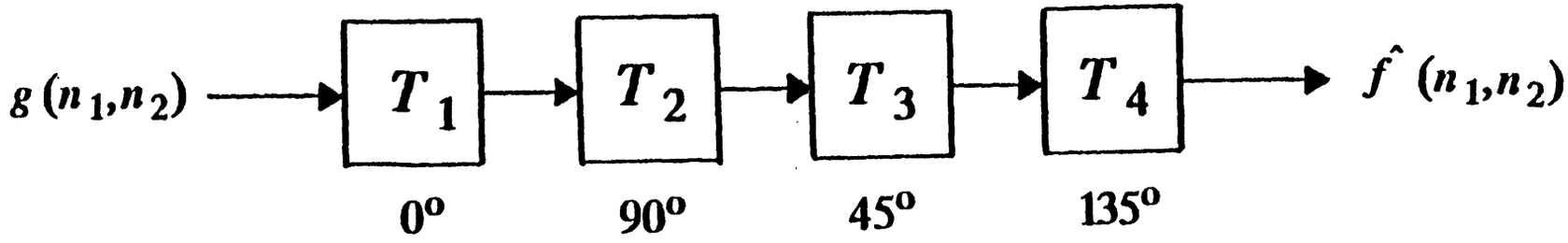

Figure 3.1 (b) The proposed 1-D approach.

The output of the system $\hat{f}(n_1,n_2)$ is then given by

$$\hat{f}(n_1,n_2) = T_4\Big[T_3\Big[T_2\Big[T_1\big[g(n_1,n_2)\big]\Big]\Big]\Big] \tag{3.2}$$

It should be noted that T_i 's are not obtained by factoring T. If they were, the system of the cascaded 1-D filters would be identical to T. The approach also does not attempt to approximate T by a cascade of T_i 's. The output of the cascaded filters may therefore be significantly different from the output of the 2-D filter.

3.4 Discussion

3.4.1 Advantages of the approach

The cascaded 1-D processing improves the existing 2-D methods without modifying the assumed image model or the basic principle of the 2-D methods. Specifically,

(1) in the flat areas, the cascaded 1-D filters is equivalent to a single 2-D filter with a much larger support size than the original 2-D filter, thus resulting in more effective noise reduction;

(2) in the edge regions, the noise near an edge is smoothed by one of the 1-D filters oriented approximately in the same direction as the edge;

(3) since the 1-D filters are adaptive and edge preserving, sequential application of the four filters does not blur the edges;

(4) the computational load of this approach is typically lighter than the corresponding 2-D filtering because of the 1-D calculations.

3.4.2 Comparison with Other 1-D Approaches

A few examples of other 1-D approaches to adaptive image restoration have been reviewed in the previous chapter. Their general principle can be summarized by Figure 3.2. The noisy image is filtered by a bank of filters whose outputs are summed, selected, or averaged to give the output of the overall system.

The parallel structure of these approaches is obviously different from the cascade structure of the present approach. More importantly, their objectives in using 1-D filters are fundamentally different. The other 1-D approaches generally aim to reduce the amount of computations by approximating the truly 2-D filters. The results are generally suboptimal compared to the truly 2-D filters, as some information in the 2-D domain is unavoidably lost in the approximation. In contrast, the goal of the present approach is to improve the performance of the 2-D filter by using 1-D filters to compensate for the lack of edge information in the 2-D filter.

Since the present approach has a cascade structure, weight calculations are not necessary. In the other approaches, the manner in which the results are combined may result in further deterioration of performance. For example, any forms of unweighted or weighted averaging would blur the edges, while selecting one output out of several would result in insufficient noise smoothing.

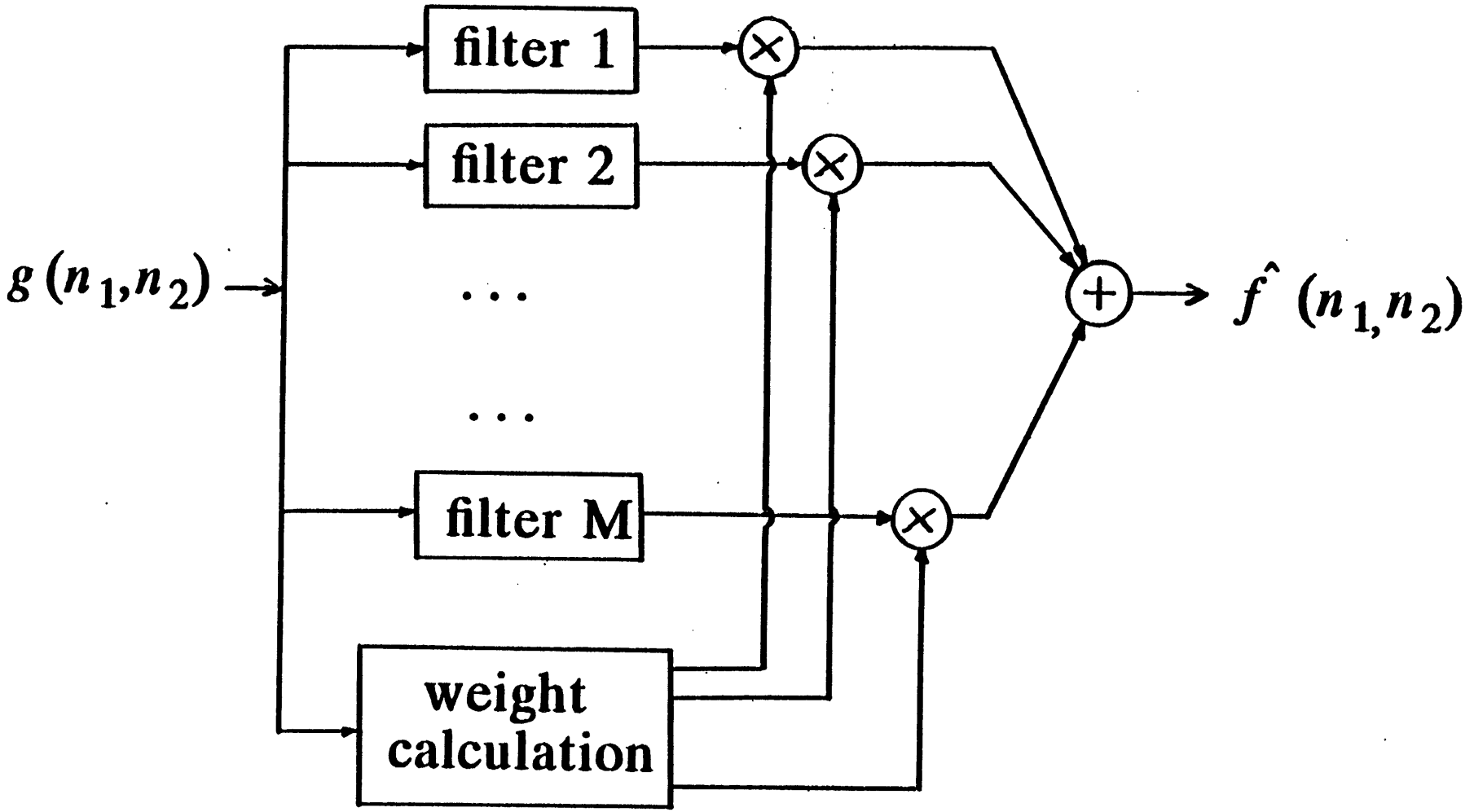

Figure 32. General block diagram of other 1-D approaches

3.4.3 Practical Considerations

Because the filterings are performed sequentially, the signal and noise characteristics change after each filtering and have to be updated before subsequent filtering. Certain assumptions may have to be made so that the same restoration principle may be used on all four filters. For example, if the principle is based on the assumption that the image and noise are not correlated, the same has to be assumed for all four filters.

Although four sequential filtering operations are involved, a large on-line memory is not required. Since each of the 1-D filters performs local filtering, the next filter may commence as soon as sufficient data are available from the previous filter. Therefore, with a moving buffer of modest size, the four filtering operations can practically be performed in parallel.

The size of each of the 1-D filters should be selected so that the 1-D filters may follow closely the contour of the edges in the image. On the other hand, it should be sufficiently large for adequate noise reduction.

The operators T_i 's are data dependent, space variant, and, therefore non-commutative. Therefore, the order in which the four 1-D filters are performed will affect the final results. For a general image with no prominent correlation in any particular direction, the different orders do not result in any significant difference in performance. However, if an image shows a lot of correlation in, say, the vertical direction, then it is preferable that the filtering in that direction be carried out first.

In applying this approach to an image restoration system, one must remember that this approach performs well because it implicitly takes into

account the orientation of the edges. Therefore, it will achieve better improvement over the 2-D approach if the latter does not model edges adequately.

3.5 Conclusion

A new 1-D approach to adaptive image restoration has been presented. The approach, motivated by the ability for 1-D filters to remove noise along an edge, aims to improve the performance of some adaptive image restoration systems which do not model edges adequately. It is different from previous 1-D approaches which typically approximate 2-D filters for computational reasons. Some specific examples of using the new approach will be given in the next chapter.

CHAPTER 4

APPLICATIONS OF THE ONE-DIMENSIONAL APPROACH

4.1 Introduction

In this chapter, three examples of applying the 1-D approach to existing 2-D image restoration systems will be presented. The restoration systems used are

(1) an adaptive filter based on local statistics of the image [5],

(2) an adaptive filter based on the noise sensitivity of human vision [6], and

(3) an adaptive filter using the spectral subtraction technique [7].

In all three examples, an image $f(n_1,n_2)$ is degraded by additive white noise. The observed image $g(n_1,n_2)$ can be represented by

$$g(n_1,n_2) = f(n_1,n_2) + w(n_1,n_2) \tag{4.1}$$

where $w(n_1,n_2)$ is a zero-mean white noise sequence assumed uncorrelated with $f(n_1,n_2)$.

The basic principle of each algorithm will be reviewed. The 1-D approach will be used to modify the algorithm, and the experimental results of restoration by both 1-D and 2-D approaches will be presented.

4.2 Adaptive Filter Based on Local Statistics

A very simple, but effective restoration algorithm was proposed by Lee [5]. In this algorithm, edges are modeled by higher local signal variance, and preserved by an adaptive filter determined from the values of the local variance and mean.

4.2.1 The 2-D LLSE Algorithm

By modeling an image $f(n_1,n_2)$ as consisting of a nonstationary mean component [18] and nonstationary and approximately white fluctuations about the mean, the linear least square error (LLSE) estimate of $f(n_1,n_2)$, based on local stationarity, is readily derived as

$$\hat{f}(n_1,n_2) = \frac{\sigma_f^2(n_1,n_2)}{\sigma_f^2(n_1,n_2)+\sigma_w^2(n_1,n_2)} [g(n_1,n_2)-m_g(n_1,n_2)] + m_f(n_1,n_2) \quad (4.2)$$

where $m_f(n_1,n_2)$ and $\sigma_f^2(n_1,n_2)$ are, respectively, the *a priori* local mean and variance of $f(n_1,n_2)$, $\sigma_w^2(n_1,n_2)$ is the local noise variance, and $m_g(n_1,n_2)$ is the mean of $g(n_1,n_2)$.

The *a priori* mean and variance of $f(n_1,n_2)$ are estimated from the observations in a $(2p+1)\times(2q+1)$ window as

$$\hat{m}_f(n_1,n_2) = \hat{m}_g(n_1,n_2) = \frac{1}{(2p+1)(2q+1)} \sum_{k_1=n_1-p}^{n_1+p} \sum_{k_1=n_2-q}^{n_2+q} g(k_1,k_2) \quad (4.3)$$

and

$$\hat{\sigma}_f^2(n_1,n_2) = \begin{cases} \hat{\sigma}_g^2(n_1,n_2)-\sigma_w^2(n_1,n_2) & \text{if } \hat{\sigma}_g^2(n_1,n_2)>\sigma_w^2(n_1,n_2) \\ 0 & \text{otherwise} \end{cases} \quad (4.4)$$

where

$$\hat{\sigma}_g^2(n_1,n_2) = \frac{1}{(2p+1)(2q+1)} \sum_{k_1=n_1-p}^{n_1+p} \sum_{k_1=n_2-q}^{n_2+q} [g(k_1,k_2)-\hat{m}_g(n_1,n_2)]^2 \qquad (4.5)$$

The LLSE algorithm can be viewed as an example of the two-channel process described in Figure 4.1. In the two-channel process, the input signal is divided into two paths: a low-pass signal (m_g) and a high-pass signal ($g-m_g$). The high-pass signal is scaled by a function of its variance, as described by Eqn. (4.2), and combined with the low-pass signal to form the output.

The filter is spatially variant and nonlinear. Its coefficients are calculated at every pixel with the window sliding in the direction of scan. Edges are preserved through the ratio of $\sigma_f^2(n_1,n_2)$ to $\sigma_w^2(n_1,n_2)$. As $\sigma_f^2(n_1,n_2)$ varies from 0 to ∞, the filter is a compromise between the simple local averaging filter and the identity filter. Thus, at high SNR regions, such as edge regions, where $\sigma_f^2(n_1,n_2)$ is much higher than $\sigma_w^2(n_1,n_2)$, the estimate is nearly equal to the observation, and little noise is removed.

The local LLSE filter preserves edges by removing less noise in the edge region than the flat region. This is acceptable if the image has a high SNR and is processed for human viewing, as the human visual system is less sensitive to noise in a busy area. However, for images with very low SNR, the unremoved noise near edges may become clearly visible. Furthermore, if the processed image is to be used for subsequent processing, rather than human viewing, it is preferable to remove noise from the edge regions as well. It will be demonstrated that by applying the 1-D approach, one can remove noise near an edge, while preserving the edge.

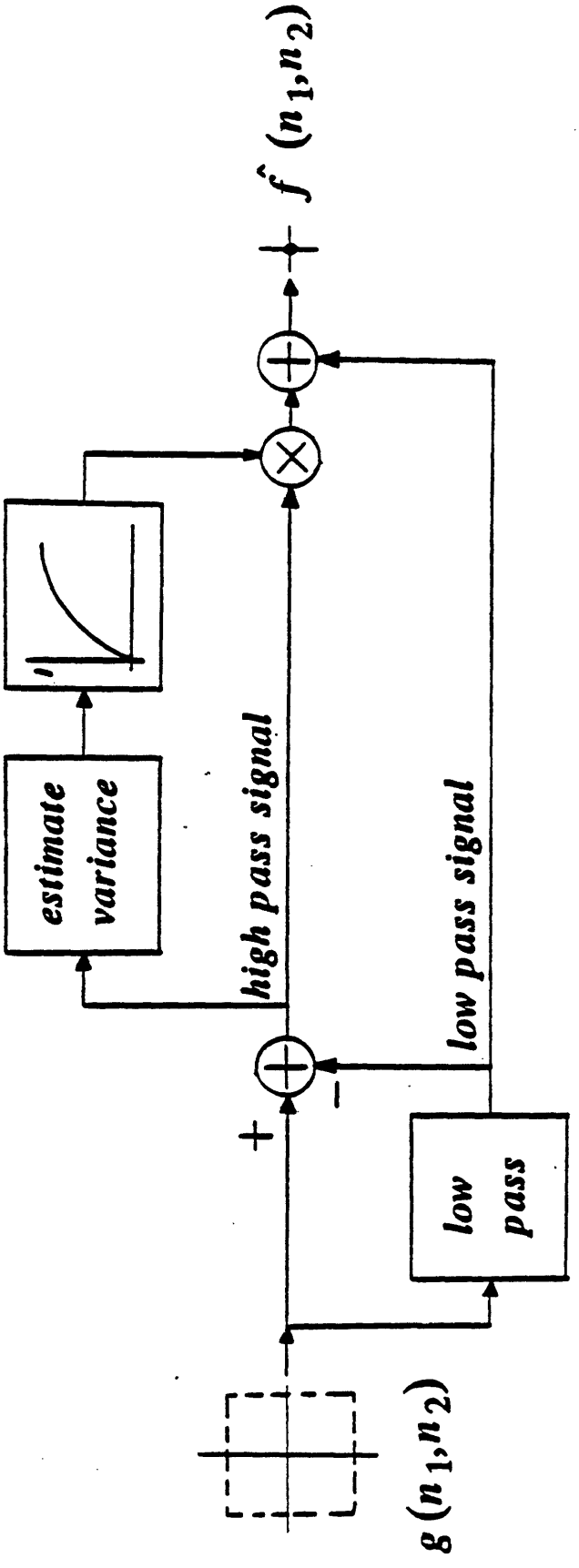

Figure 4.1 General block diagram of a restoration technique based on local statistics.

4.2.2 The 1-D LLSE Algorithm

Consider a 1-D spatially variant filter oriented in the horizontal direction and implemented using the same principle as the LLSE algorithm. The output of the 1-D filter is

$$\hat{f}_1(n_1,n_2) = \frac{\hat{\sigma}_f^2(n_1,n_2)}{\hat{\sigma}_f^2(n_1,n_2)+\sigma_w^2(n_1,n_2)} [g(n_1,n_2)-\hat{m}_g(n_1,n_2)] + \hat{m}_f(n_1,n_2) \quad (4.6)$$

where the mean and variance estimates are calculated from

$$\hat{m}_f(n_1,n_2) = \hat{m}_g(n_1,n_2) = \frac{1}{(2p+1)} \sum_{k_1=n_1-p}^{n_1+p} g(k_1,n_2) \quad (4.7)$$

and

$$\hat{\sigma}_f^2(n_1,n_2) = \begin{cases} \hat{\sigma}_g^2(n_1,n_2)-\sigma_w^2(n_1,n_2) & \text{if } \hat{\sigma}_g^2(n_1,n_2)>\sigma_w^2(n_1,n_2) \\ 0 & \text{otherwise} \end{cases} \quad (4.8)$$

where

$$\hat{\sigma}_g^2(n_1,n_2) = \frac{1}{(2p+1)} \sum_{k_1=n_1-p}^{n_1+p} [g(k_1,n_2)-\hat{m}_g(n_1,n_2)]^2 \quad (4.9)$$

The second 1-D filter, say, the vertical filter, is obtained in a similar way and applied to $\hat{f}_1(n_1,n_2)$. We note, however, that the noise term $\sigma_w^2(n_1,n_2)$ should be updated as the first filter has reduced the noise power. Thus, if $h_1(k_1; n_1,n_2)$ represents the unit sample response of the first filter at (n_1,n_2), we can estimate the reduced noise power at each pixel, (n_1,n_2), as

$$\sigma_{w_1}^2(n_1,n_2) = \sum_{k_1=n_1-p}^{n_1+p} h_1^2(k_1; n_1,n_2)\, \sigma_w^2(k_1,n_2) \quad (4.10)$$

Extension to the two remaining 1-D filters at 45 and 135 degrees is similar.

The resulting system is a cascade of 1-D filters capable of adapting to the edge orientation in the image, whereas the 2-D filter discussed earlier is insensitive to edge orientation. Thus, a sharp edge inclined at a large angle to the filtering direction remains practically intact, while the noise at the edge is removed by one of the filters oriented closest to the direction of the edge. The 1-D approach also performs better in low contrast regions. If the 1-D filters are each of length M, the cascaded filters are in effect an octagonal filter with sides of length M and a filter support of size $7M^2-10M+4$. This is considerably larger than M^2 for a $M \times M$ 2-D filter, and more effective in noise reduction. The objective and subjective improvement in performance over the 2-D LLSE filter will be shown in the next section.

4.2.3 EXPERIMENTAL RESULTS

This section presents experimental results where both 2-D and 1-D filtering techniques, discussed in the previous sections, were applied to restore images degraded by additive white noise. In the 1-D method, the image was filtered horizontally (0°), vertically (90°), along the (45°) angle, and finally along the (135°) angle. The window sizes were chosen as 5×5 and 5×1, respectively, in the 2-D and 1-D methods for the best tradeoff between noise removal and resolution.

Figures 4.2 and 4.3 illustrate the behavior of the two filters near an edge. Figure 4.2(a) shows an image, consisting of two flat regions separated by a vertical edge. The image is degraded by noise, as shown in Figure 4.2(b). The

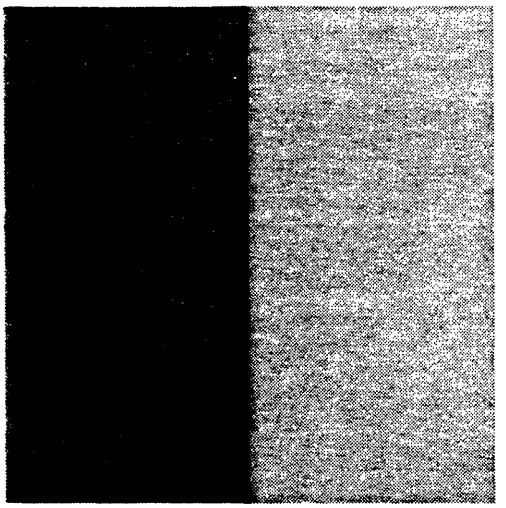

(a)

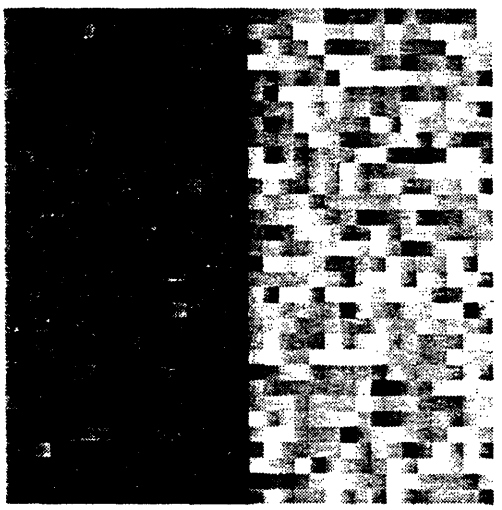

(b)

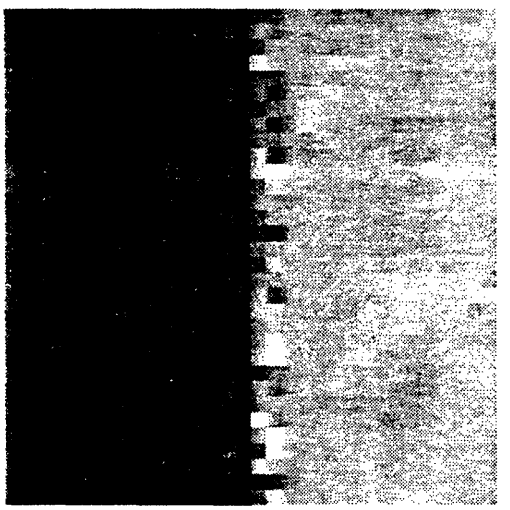

(c)

Figure 4.2 (a) Original image.

(b) Noisy image.

(c) Image in (b) restored by the 2-D LLSE algorithm.

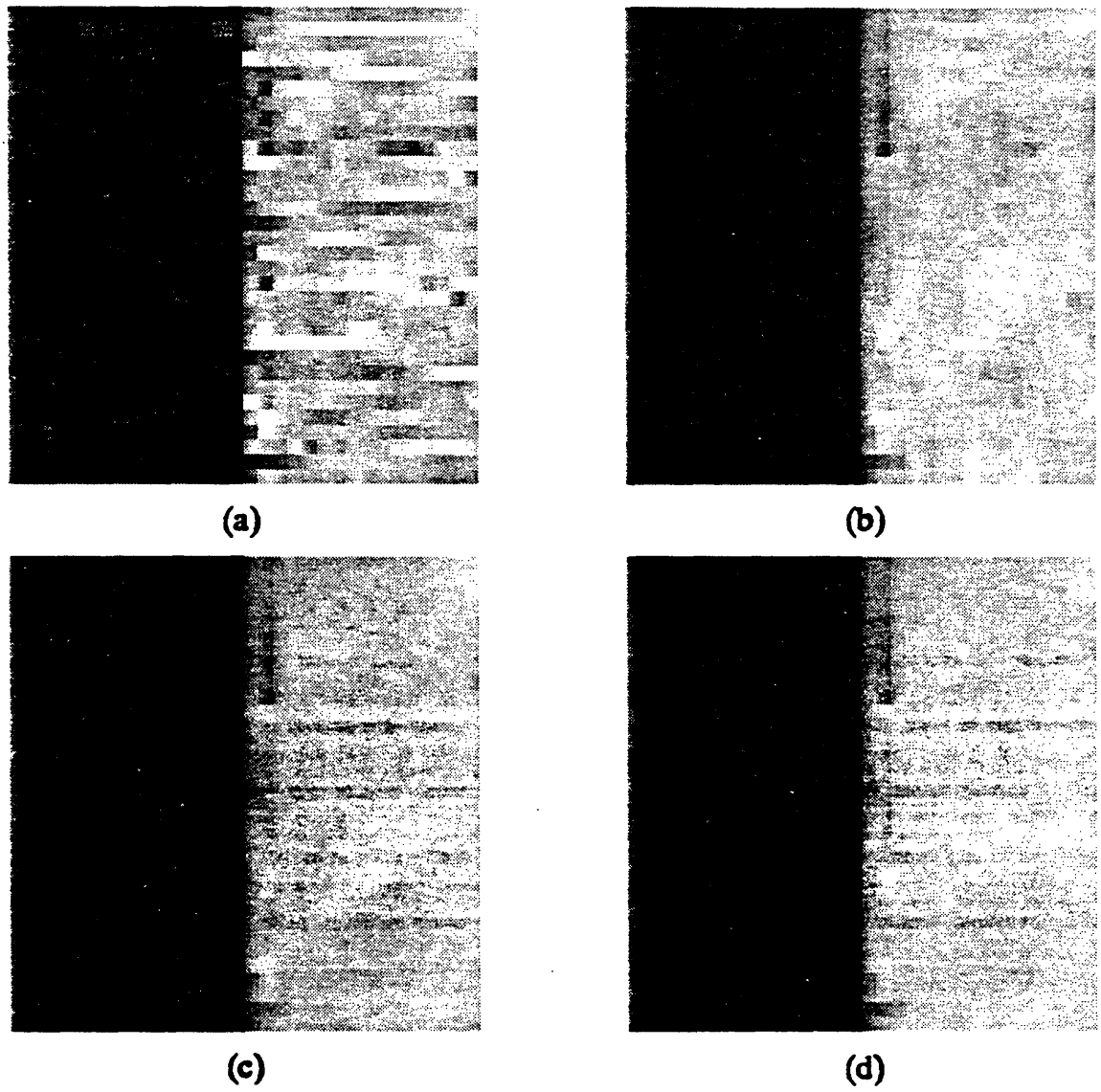

Figure 43 (a) Figure 42(b) processed by the horizontal filter.

(b) Image in (a) processed by the vertical filter.

(c) Image in (b) processed by the 45-degree filter.

(d) Image in (c) processed by the 135-degree filter.

result of 2-D filtering, as shown in Figure 4.2(c), indicates practically no noise smoothing near the edge. Figure 4.3 shows that the noise near the edge is reduced by the vertical 1-D filter, while the edge is not blurred by the other three filters. Figure 4.3(d) also shows more noise reduction in the flat regions than that achieved by the 2-D method.

The results of processing real images are shown in Figures 4.6 and 4.7. Two images of the 'BANK' and the 'GIRL', which have different correlation characteristics, are chosen. The original pictures, each with 256×256 8-bit pixels, are shown in Figures 4.4(a) and 4.5(a). The images were degraded by additive white Gaussian noise at various SNRs. The SNR of an image, say $g(n_1,n_2)$, is defined as

$$\text{SNR} = 10 \log \frac{\sum\sum_{n_1 n_2} [g(n_1,n_2) - f(n_1,n_2)]^2}{\sum\sum_{n_1 n_2} [f(n_1,n_2) - m_f]^2} \tag{4.11}$$

where m_f is the mean of the original image $f(n_1,n_2)$. Two degraded images at a SNR of 10 dB are shown in Figures 4.4(b) and 4.5(b). In both methods, the noise variance was estimated from a window of about 1500 pixels in a flat area of the degraded image.

The results are summarized in Table 1, which lists the improvement in SNR, for input SNRs ranging from 0 dB to 10 dB.

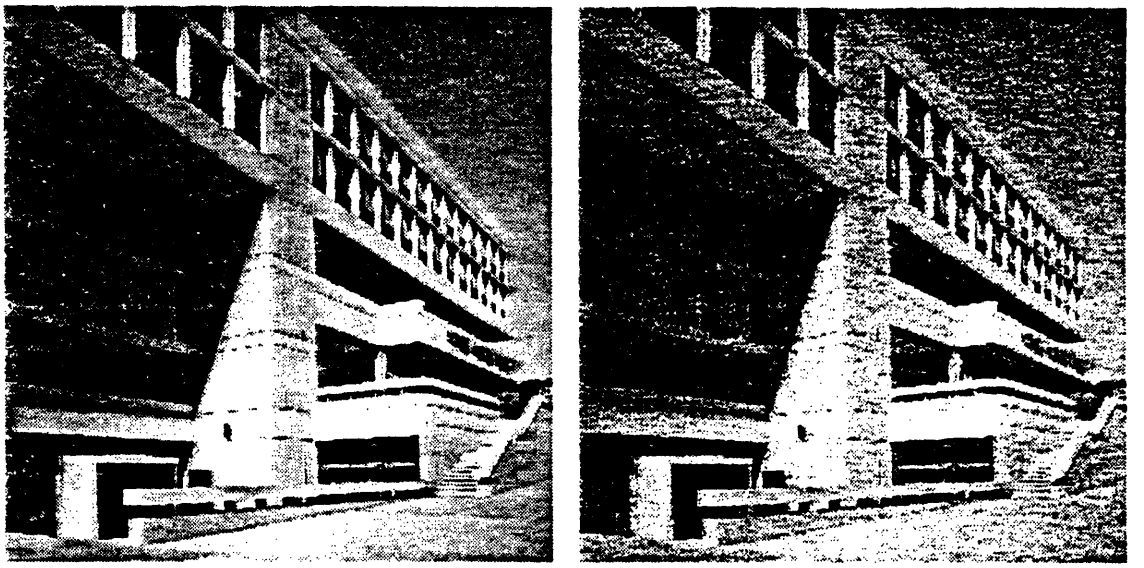

(a) (b)

Figure 4.4 (a) Original 'BANK' image.

(b) 'BANK' image degraded by additive noise at 10dB SNR.

(a) (b)

Figure 4.5 (a) Original 'GIRL' image.

(b) 'GIRL' image degraded by additive noise at 10dB SNR.

Table 4.1: SNR improvement: 2-D vs 1-D LLSE algorithms

Input SNR (dB)	Improvement (dB)			
	'BANK' Image		'GIRL' Image	
	2-D filter	1-D filter	2-D filter	1-D filter
0	6.64	7.61	8.66	9.31
3	6.09	6.94	7.80	8.14
6	5.46	6.17	6.79	7.28
10	4.47	4.99	5.53	5.74

Quantitatively, 1-D filtering results in up to 1 dB improvement over 2-D filtering. The improvement is more significant for the 'BANK' image, which possesses more distinctive correlation in the four directions considered. The improvement in visual quality can be seen in figures 4.6 and 4.7. Figures 4.6(a) and 4.7(a) show the results of the 2-D method, and figures 4.6(b) and 4.7(b) show the results of the 1-D method. The 2-D filtering preserves edges, but does so at the expense of insufficient noise removal, particularly in the edge regions. Images restored by the 1-D approach show its superiority in preserving edges and reducing noise in all regions, including the edge areas. This is shown more clearly in Figures 4.8 and 4.9, which are enlarged segments of Figures 4.4 - 4.7. These results indicate that the 1-D filtering is more effective in both high and low contrast regions.

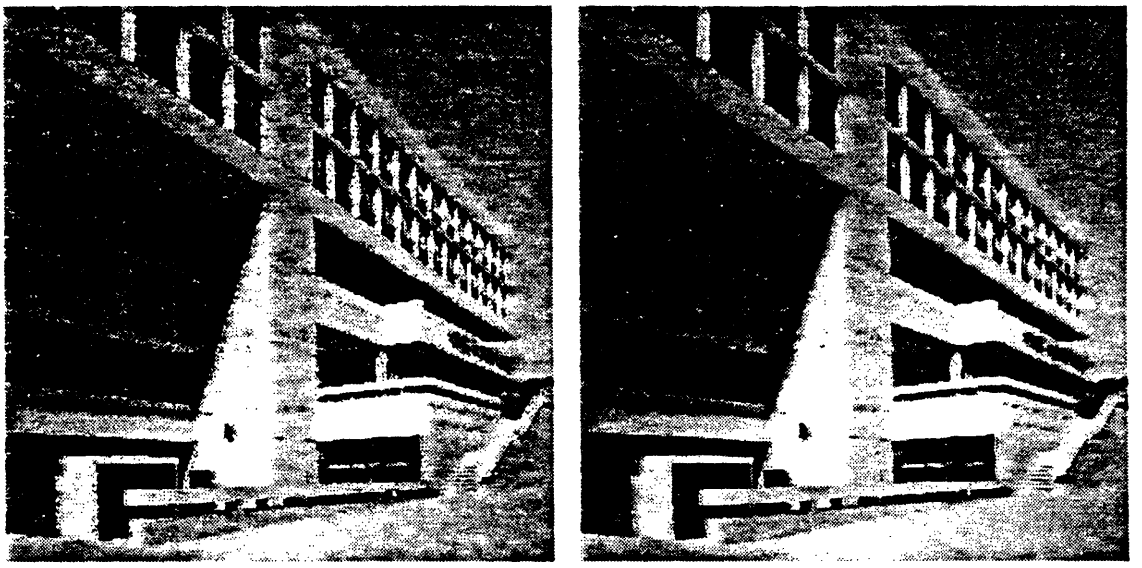

(a) (b)

Figure 4.6 (a) Figure 4.4(b) restored by the 2-D LLSE algorithm.
(b) Figure 4.4(b) restored by the 1-D LLSE algorithm.

(a) (b)

Figure 4.7 (a) Figure 4.5(b) restored by the 2-D LLSE algorithm.
(b) Figure 4.5(b) restored by the 1-D LLSE algorithm.

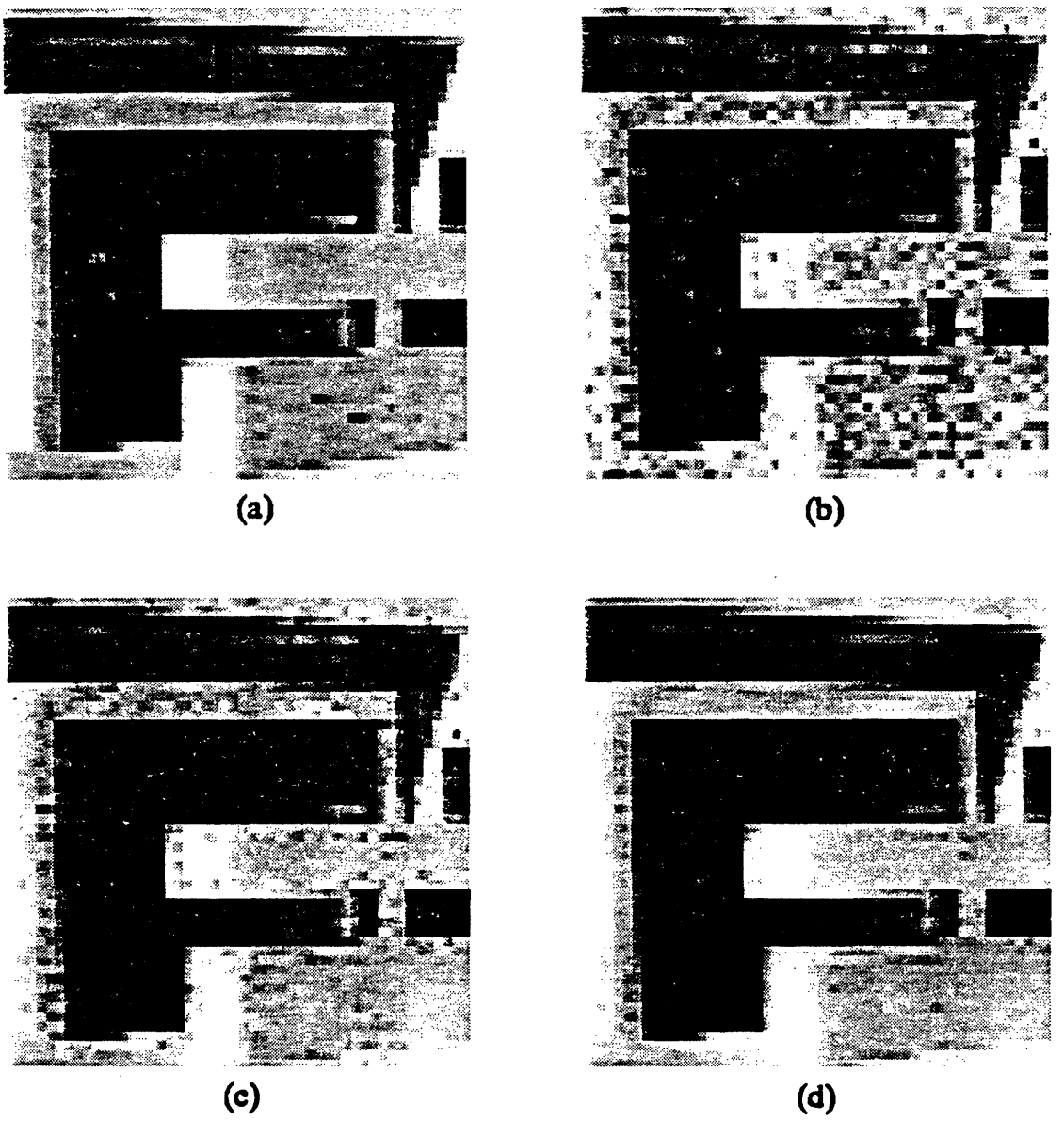

Figure 4.8 (a) An enlarged section of figure 4.4(a).

(b) An enlarged section of figure 4.4(b).

(c) An enlarged section of figure 4.6(a).

(d) An enlarged section of figure 4.6(b).

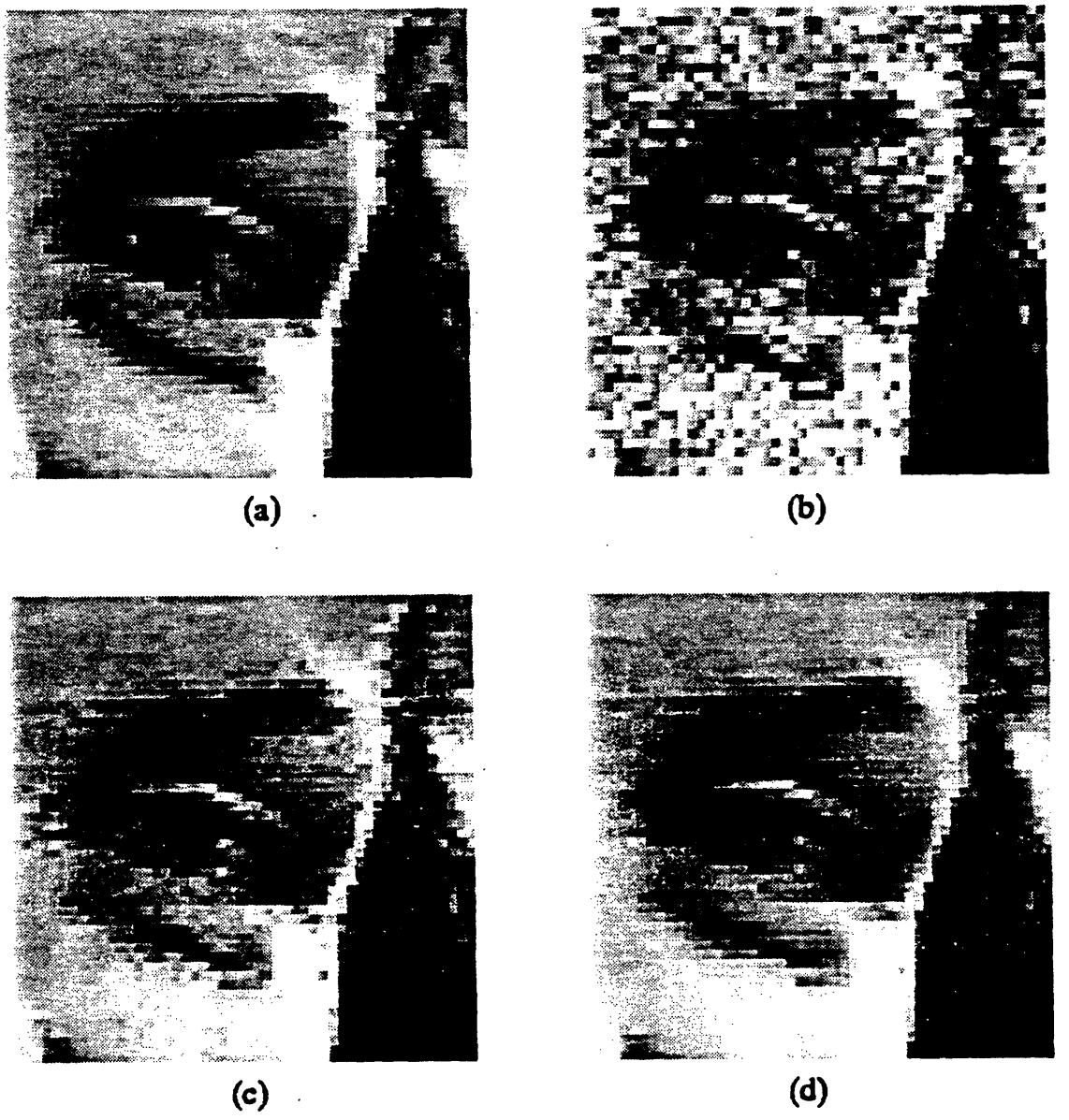

Figure 4.9 (a) An enlarged section of figure 4.5(a).

(b) An enlarged section of figure 4.5(b).

(c) An enlarged section of figure 4.7(a).

(d) An enlarged section of figure 4.7(b).

4.3 Adaptive Filter Based on a Noise Visibility Function

The sensitivity of the human visual system to noise in an image decreases with the amount of local spatial details. In other words, the sensitivity is highest in the flat areas, and lowest in the busy areas. This effect is incorporated in a restoration system proposed by Anderson and Netravali [6]. They quantified the noise sensitivity by a 'visibility function', which represents a subjective tradeoff between resolution and noise. Using this 'visibility function' they constructed a performance index, which leads to an adaptive filter (called the S-type filter) capable of maintaining the tradeoff between the noise removed and the blur introduced by the filter. This section describes further improvement to this algorithm by the 1-D approach.

4.3.1 The 2-D S-type Filter

The Visibility Function

A 'masking function', $M(n_1,n_2)$, at a pixel (n_1,n_2) is defined as a measure of spatial detail at the pixel:

$$M(n_1,n_2) = \sum_{k_1=n_1-p}^{n_1+p} \sum_{k_2=n_2-q}^{n_2+q} C^{\|(n_1,n_2)-(k_1,k_2)\|} [|m_h(k_1,k_2)| + |m_v(k_1,k_2)|] \qquad (4.12)$$

where $\|(n_1,n_2)-(k_1,k_2)\|$ denotes the Euclidean distance between (n_1,n_2) and (k_1,k_2); $m_h(k_1,k_2)$ and $m_v(k_1,k_2)$ are, respectively, the horizontal and vertical slopes of the image intensity at (k_1,k_2); C is a constant (taken as 0.35). Note that $M(n_1,n_2)$ increases monotonically with the amount of spatial detail in a neighborhood surrounding (n_1,n_2).

A subjective test was conducted to determine a 'visibility function', $F(n_1,n_2)$, which gives the relative visibility of a unit of noise added to all parts in the image where $M(n_1,n_2)$ has a certain value. In other words, the subjective 'noise visibility' at a point where $F = F_0$ is equal to that at another point where $F = \frac{1}{2}F_0$ and the amount of noise is doubled. It was found that $F(n_1,n_2)$ can be approximated by a decreasing function of $M(n_1,n_2)$ as

$$F(n_1,n_2) = e^{-\beta M(n_1,n_2)} \tag{4.13}$$

for some appropriate value of β.

The Restoration Filter

Let the impulse response of the 2-D spatial variant filter be $h(k_1,k_2;n_1,n_2)$, where

$$h(k_1,k_2;n_1,n_2) \begin{cases} \neq 0 & -q \le k_1 \le q, -q \le k_2 \le q \\ = 0 & \text{otherwise} \end{cases} \tag{4.14}$$

It is desired that the filter removes as much noise as possible. On the other hand, the filter must also introduce little blurring. The former is measured by the relative amount of noise passed, v_a, given by

$$v_a(n_1,n_2) = \sum_{k_1=-q}^{q} \sum_{k_2=-q}^{q} h^2(k_1,k_2;n_1,n_2) \tag{4.15}$$

and the latter is quantified by the spread function

$$w_a(n_1,n_2) = \sum_{k_1=-q}^{q} \sum_{k_2=-q}^{q} h^2(k_1,k_2;n_1,n_2) \cdot (k_1^2 + k_2^2) \tag{4.16}$$

Since the two requirements are somewhat contradictory, the optimal filter is obtained by minimizing the joint objective function

$$J(n_1,n_2) = \alpha v_a(n_1,n_2) + (1-\alpha) w_a(n_1,n_2) \tag{4.17}$$

subject to the constraint

$$\sum_{k_1=-q}^{q} \sum_{k_2=-q}^{q} h(k_1,k_2;n_1,n_2) = 1 \tag{4.18}$$

where α $(0 \le \alpha \le 1)$ is a tuning parameter. Using the Lagrange multiplier λ, the sclution is given by

$$h(k_1,k_2;n_1,n_2) = \begin{cases} \dfrac{\lambda}{\alpha + (1-\alpha)(k_1^2 + k_2^2)} & -q \le k_1 \le q, -q \le k_2 \le q \\ 0 & \text{otherwise} \end{cases} \tag{4.19}$$

where λ is adjusted so that the constraint (4.18) is satisfied.

The Role of $F(n_1,n_2)$

The filter is determined so that in flat areas, it approaches an averaging filter, and in edge areas, it approaches the identity filter. This is achieved by tuning α so that the amount of 'visible noise' is a constant. More specifically, let ϕ determine the relative amount of noise passed by the filter in a perfectly flat area, where $M(n_1,n_2)=0$ and $F(n_1,n_2)=1$. The value of ϕ is chosen from the range between $\dfrac{1}{(2q+1)^2}$ (corresponding to a $(2q+1)\times(2q+1)$ averaging filter) and 1 (corresponding to an identity filter), and held constant over the entire image. At a pixel where $M(n_1,n_2)>0$, set α so that the 'visible noise' at the pixel is

$$v_a(n_1,n_2)F^{\gamma}(n_1,n_2) = \phi \tag{4.20}$$

where γ is another tuning parameter. The parameter γ is held constant over the entire image, for more control on the response of the filter to the 'visibility function'. We note that v_a increases as M increases.

The algorithm to determine the filter is, therefore,

(1) Choose a value of ϕ and a value of γ.

(2) Determine $M(n_1,n_2)$ and $F(n_1,n_2)$ by Eqn. (4.12) and Eqn. (4.13).

(3) Solve Eqn. (4.20) for $v_a(n_1,n_2)$.

(4) Iteratively adjust α and determine $h(k_1,k_2;n_1,n_2)$ by Eqn. (4.19) until Eqn. (4.15) is satisfied.

(5) Repeat steps (2)-(4) for all (n_1,n_2) in the image.

We note that the impulse response $h(k_1,k_2;n_1,n_2)$ is isotropic, and changes its shape with the amount of local detail. Thus, at points of high detail, the response is peaked, and in the flat area, the response is flat. Details in the image are therefore preserved, and the noise in the flat areas is removed. Although the algorithm does not explicitly require knowledge about the noise, the value of γ that gives the best performance is influenced by the amount of noise present via the masking function $M(n_1,n_2)$. More specifically, for images of low SNR's, the value of γ will have to be tuned down to achieve better noise smoothing.

4.3.2 The 1-D S-type Filter

Consider a 1-D filter oriented in the horizontal direction and designed using the same principle as the S-type filter. The impulse response of the 1-D horizontal S-type filter is given by

$$h_1(k_1; n_1, n_2) = \begin{cases} \dfrac{\lambda}{\alpha + (1-\alpha) k_1^2} & -q \le k_1 \le q \\ 0 & \text{otherwise} \end{cases} \tag{4.21}$$

The procedure to determine the filter coefficients is similar to that in the 2-D case. For example, the horizontal masking function is calculated by

$$M_1(n_1, n_2) = \sum_{k_1 = n_1 - p}^{n_1 + p} C^{\,||(n_1, n_2) - (k_1, n_2)||} \, |m_h(k_1, n_2)| \tag{4.22}$$

The noisy image is then filtered by $h_1(k_1; n_1, n_2)$. The resulting image is filtered sequentially in the other three directions by the other three 1-D filters, each determined in a similar manner.

4.3.3 Experimental Results

The same 'BANK' and 'GIRL' images used in the previous example are used to illustrate the effectiveness of the 1-D S-type filter. The window sizes were again chosen as 5×5 and 5×1 for the 2-D and 1-D algorithms, respectively. The value of β in Eqn. (4.13) was chosen as 0.02, so that the visibility function is similar to that given by [6]. The parameter ϕ was chosen as 0.04 and 0.2, respectively, for the 2-D and 1-D algorithms. In both algorithms, the values of the

masking function $M(n_1,n_2)$ were estimated from the original noiseless image because estimating $M(n_1,n_2)$ from the noisy image is unreliable (as noted in [6]), especially for images of very low SNR's. Although better ways of estimating $M(n_1,n_2)$ from the noisy data have been proposed (see [16], for example), noiseless estimate of $M(n_1,n_2)$ was used for the purpose of comparing the 2-D and 1-D algorithms. Since the performance of the algorithms depends on the value of γ selected, the value of γ for each image was adjusted until the best SNR improvement was obtained.

The results are summarized in Table 4.2 for various input SNRs.

Table 4.2: SNR improvement: 2-D vs 1-D S-type filters

Input SNR (dB)	Improvement (dB)			
	'BANK' Image		'GIRL' Image	
	2-D filter	1-D filter	2-D filter	1-D filter
0	8.09	9.33	9.55	10.50
3	7.42	8.83	8.97	9.79
6	6.43	7.96	8.00	8.74
10	5.03	6.66	6.53	7.17

Similar to the LLSE algorithm in section 4.2, the 1-D S-type filter performs better than the 2-D S-type filter. In terms of SNR, the 1-D filter results in 0.6 to

1.5 dB improvement over the 2-D filter. The improvement is again more significant for the 'BANK' image. Figures 4.10 and 4.11 show the results of restoring the degraded 'BANK' and 'GIRL images at an SNR of 10 dB (see Figures 4.4 and 4.5). The 2-D filter does not result in sufficient noise smoothing in both the flat areas and the edge areas, as shown in Figures 4.10(a) and Figure 4.11(a). This is improved by the 1-D filter, as shown in Figures 4.10(b) and 4.11(b).

4.4 Short Space Spectral Subtraction Technique

Image restoration in the frequency domain faces the problem of estimating the power spectral density, $P_f(\omega_1,\omega_2)$, of the original image $f(n_1,n_2)$, from the noisy observation. Lim [7], using a particular method of expressing $P_f(\omega_1,\omega_2)$ as a function of $f(n_1,n_2)$, proposed a spectral subtraction scheme for estimating $f(n_1,n_2)$ directly from $g(n_1,n_2)$. The algorithm is implemented on a short space basis, in which the degraded image is divided into many subimages. Each subimage is restored separately, and the subimages are then combined.

4.4.1 The 2-D Short Space Spectral Subtraction Technique

A short space window $r_{ij}(n_1,n_2)$ is first applied to $g(n_1,n_2)$. The windowed observation $g_{ij}(n_1,n_2)$ is related to the windowed image $f_{ij}(n_1,n_2)$ and the windowed noise $w_{ij}(n_1,n_2)$ by

$$g_{ij}(n_1,n_2) = f_{ij}(n_1,n_2) + w_{ij}(n_1,n_2) \tag{4.23}$$

Then, by subtracting the noise spectrum from the spectrum of the noisy observation, the estimate of $F_{ij}(\omega_1,\omega_2)$ is given by

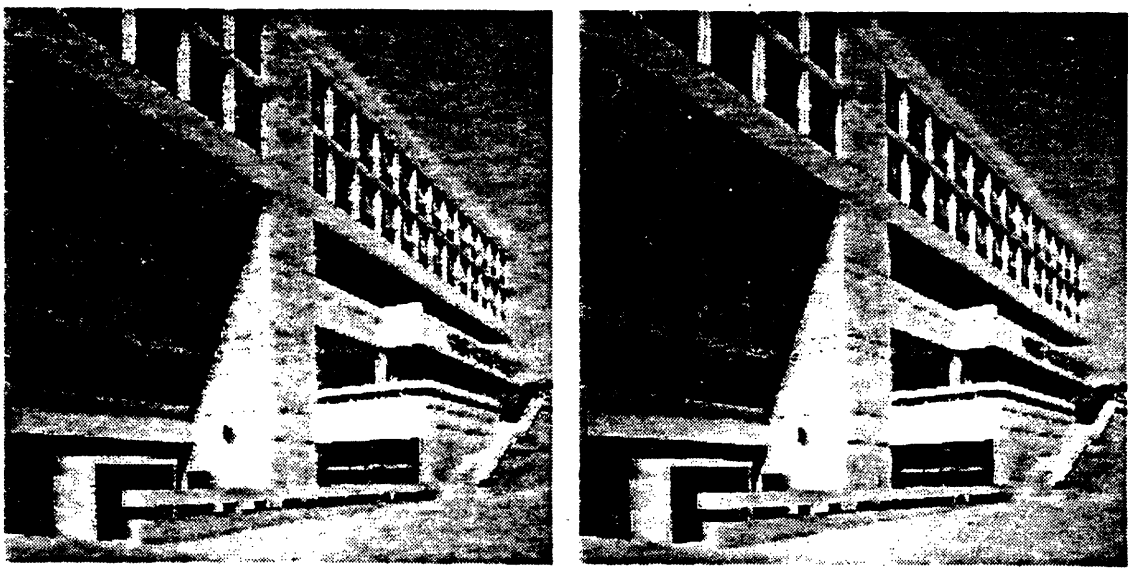

(a) (b)

Figure 4.10 (a) Figure 4.4(b) restored by the 2-D S-type filter.

(b) Figure 4.4(b) restored by the 1-D S-type filter.

(a) (b)

Figure 4.11 (a) Figure 4.5(b) restored by the 2-D S-type filter.

(b) Figure 4.5(b) restored by the 1-D S-type filter.

$$|\hat{F}_{ij}(\omega_1,\omega_2)| = \begin{cases} [|G_{ij}(\omega_1,\omega_2)|^2 - \alpha \cdot k \cdot P_w(\omega_1,\omega_2)]^{1/2} \\ \qquad \text{if } |G_{ij}(\omega_1,\omega_2)|^2 > \alpha \cdot k \cdot P_w(\omega_1,\omega_2) \\ 0 \qquad \text{otherwise} \end{cases} \tag{4.24}$$

and

$$\measuredangle \hat{F}_{ij}(\omega_1,\omega_2) = \measuredangle G_{ij}(\omega_1,\omega_2) \tag{4.25}$$

where $P_w(\omega_1,\omega_2)$ is the power spectral density of the noise, assumed uniform over the image. The parameter α determines the amount of subtraction, and can be adjusted to give the best performance. The constant k normalizes the power and energy spectral density, and is given by

$$k = \sum_{n_1}\sum_{n_2} r_{ij}^2(n_1,n_2) \tag{4.26}$$

The estimate $\hat{f}(n_1,n_2)$ is then constructed by combining $\hat{f}_{ij}(n_1,n_2)$ as follows:

$$\hat{f}(n_1,n_2) = \sum_i \sum_j \hat{f}_{ij}(n_1,n_2) \tag{4.27}$$

The window $r_{ij}(n_1,n_2)$ therefore must satisfy the requirement that

$$\sum_i \sum_j r_{ij}(n_1,n_2) = 1, \qquad \text{for all } (n_1,n_2) \text{ of interest.} \tag{4.28}$$

4.4.2 The 1-D Short Space Spectral Subtraction Technique

To use the same spectral subtraction principle for the design of 1-D filters, 1-D windows and 1-D spectra are used. For example, in the horizontal filter, a 1-D window $r_{1,ij}(n_1)$ is used to window the data. The first estimate of $f_{ij}(n_1,n_2)$ is given by

$$|\hat{F}_{1,ij}(\omega_1)| = \begin{cases} [|G_{ij}(\omega_1)|^2 - \alpha \cdot k_1 \cdot P_w(\omega_1)]^{1/2} & \text{if } |G_{ij}(\omega_1)|^2 > \alpha \cdot k_1 \cdot P_w(\omega_1) \\ 0 & \text{otherwise} \end{cases} \tag{4.29}$$

and

$$\measuredangle \hat{F}_{1,ij}(\omega_1) = \measuredangle G_{ij}(\omega_1) \tag{4.30}$$

where

$$k_1 = \sum_{n_1} r^2_{1,ij}(n_1) \tag{4.31}$$

The results from the various windows are combined to form the output of the horizontal filter, as in Eqn. (4.27).

The second filter, say, the vertical filter, may be applied in a similar manner. However, the noise spectrum has to be updated because of the first filter. Specifically, the new noise spectrum can be approximated as

$$P_{w_1 ij}(\omega_1) = P_w(\omega_1) \; |H_{1,ij}(\omega_1)|^2 \tag{4.32}$$

where $H_{1,ij}(\omega_1)$ is the frequency response of the first filter given by

$$H_{1,ij}(\omega_1) = \begin{cases} \dfrac{[|G_{ij}(\omega_1)|^2 - \alpha \cdot k_1 \cdot P_w(\omega_1)]^{1/2}}{|G_{ij}(\omega_1)|} & \text{if } |G_{ij}(\omega_1)|^2 > \alpha \cdot k_1 \cdot P_w(\omega_1) \\ 0 & \text{otherwise} \end{cases} \tag{4.33}$$

Extension to the other two filters is similar.

4.4.3 Experimental Results

The 2-D and 1-D methods were applied to the 'BANK' and 'GIRL' images. The subimage sizes were chosen as 16×16 and 16×1, respectively. Separable triangular windows were used for the 2-D method, and triangular windows were used for the 1-D method. To simplify calculations, the noise at the output of each 1-D filter was assumed white. The SNR improvements are summarized in Table 4.3. In obtaining these results, the subtraction factor α was adjusted to obtain the best SNR improvement for any particular input SNR. The values of α are different for the 2-D and 1-D algorithms and range from 1.5 for an input SNR of 10 dB to 4.0 for an input SNR of 0dB.

Table 4.3: SNR improvement: 2-D vs 1-D spectral subtraction techniques

Input SNR (dB)	Improvement (dB)			
	'BANK' Image		'GIRL' Image	
	2-D filter	1-D filter	2-D filter	1-D filter
0	7.65	7.25	9.45	9.87
3	7.03	6.27	8.71	8.68
6	6.05	5.19	7.51	7.36
10	4.73	3.85	5.99	5.69

As shown in Table 4.3, the 1-D technique does not result in better SNR than the 2-D technique. Examples of restoration of images at an input SNR of 10 dB are shown in Figures 4.12 and 4.13. The results by 2-D spectral subtraction in Figures 4.12(a) and 4.13(a) clearly show its ability to preserve edges and details. Look, for example, at the vertical lines on the wall above the window in the 'BANK' picture, and the hair in the 'GIRL' picture. This indicates that the 2-D spectrum as estimated by the spectral subtraction technique can model the edges very well. As expected, the 1-D spectrum as estimated by the 1-D approach does not contain as much edge information as the 2-D spectrum, and therefore, its ability to preserve edges is inferior to the 2-D technique. On the other hand, we notice the presence of a harmonic pattern in Figures 4.12(a) and 4.13(a). This, as explained by [19], is due to the presence of a few narrowband peaks of large amplitude in the residue after the spectral subtraction. The amount of this type of artifacts is reduced by the 1-D technique, as shown in Figures 4.12(b) and 4.13(b).

This example illustrates a limitation of the 1-D approach, as explained in Chapter 3. Specifically, if the 2-D approach is based on an accurate model of the edges, the 1-D approach is not likely to improve its edge preserving ability.

4.5 Summary and Conclusion

In this chapter, three existing 2-D adaptive image restoration techniques were reviewed. In each case, the 1-D approach was applied, using the same principle as in the 2-D technique. Significant improvement was achieved by the 1-D approach in the first two examples, namely, the adaptive filter based

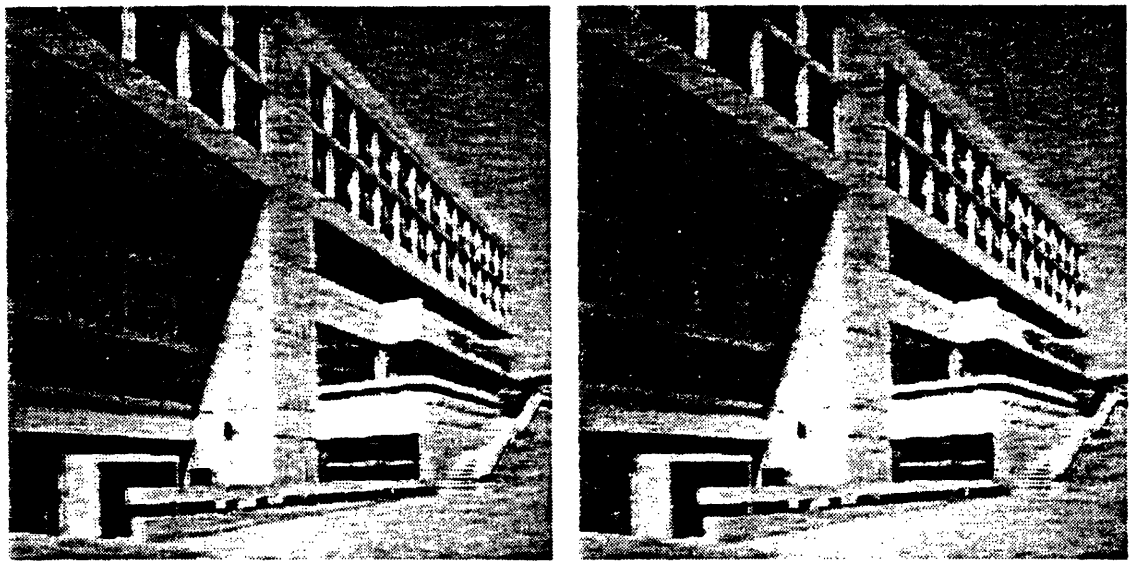

(a) (b)

Figure 4.12 (a) Figure 4.4(b) restored by the 2-D spectral subtraction technique.

(b) Figure 4.4(b) restored by the 1-D spectral subtraction technique

(a) (b)

Figure 4.13 (a) Figure 4.5(b) restored by the 2-D spectral subtraction technique.

(b) Figure 4.5(b) restored by the 1-D spectral subtraction technique.

on local statistics and the adaptive filter based on subjective noise visibility. In these examples, the edges were not adequately modeled, and the 2-D filters were therefore isotropic. The sequence of four 1-D filters in four directions compensated for this inadequacy in the model, and improved the noise smoothing capability near the edges.

In the third example, the 2-D spectral subtraction technique showed its superiority in preserving edges and details, as the 2-D spectrum could accurately describe the edges and details. No improvement, measured in terms of SNR, was achieved by the 1-D approach. However, the 1-D approach was shown to reduce the amount of artifacts present in the images restored by the 2-D technique.

From these results, it can be concluded that the 1-D approach can improve the performance of some image restoration systems which do not model edges adequately. The improvement is achieved by better noise reduction in the flat regions as well as in the edge regions, while the resolution of the image is not sacrificed.

CHAPTER 5

FURTHER APPLICATIONS OF THE ONE-DIMENSIONAL APPROACH

5.1 Introduction

The 1-D approach developed in Chapter 3 is suitable for restoring images degraded by additive noise. Specific examples were shown in the previous chapter to illustrate its effectiveness. This chapter deals with the application of the restoration techniques based on the 1-D approach to three other specific restoration problems, namely,

(1) the restoration of images degraded by blurring as well as additive noise,

(2) the restoration of images degraded by multiplicative noise, and

(3) the reduction of quantization noise in pulse code modulation image coding.

One approach to solving these problems is to transform the specific problem into one which is suitable for filtering techniques designed for reducing additive noise. In each of these applications, a noise reduction system for additive noise is incorporated as a part of the overall system. In particular, the 1-D LLSE algorithm developed in section 4.2 will be used, because it is effective in reducing noise without sacrificing the resolution of the image.

In subsequent sections, each of the applications will be examined, and the experimental results presented.

5.2 Restoration of Blurred and Noisy Images

5.2.1 The Principle of Inverse Filtering

If an image is blurred by an imaging system, which is characterized by its point spread function $h(n_1,n_2)$, the image formation can be described by

$$G(\omega_1,\omega_2) = H(\omega_1,\omega_2)\, F(\omega_1,\omega_2) \tag{5.1}$$

One simple way to estimate the original image $f(n_1,n_2)$ is to inverse filter $g(n_1,n_2)$, i.e.,

$$\hat{F}(\omega_1,\omega_2) = \frac{G(\omega_1,\omega_2)}{H(\omega_1,\omega_2)} \tag{5.2}$$

provided $H(\omega_1,\omega_2)$ has no singularity for all frequencies (ω_1,ω_2). However, in the presence of additive noise $w(n_1,n_2)$, as shown in Figure 5.1(a), the estimate is given by

$$\hat{F}(\omega_1,\omega_2) = F(\omega_1,\omega_2) + \frac{W(\omega_1,\omega_2)}{H(\omega_1,\omega_2)} \tag{5.3}$$

As $H(\omega_1,\omega_2)$ becomes small at certain spatial frequencies, its inverse becomes large, while the noise $W(\omega_1,\omega_2)$ may not be negligible at these frequencies. This results in an amplification of the noise, and the restored image is generally unsatisfactory. Therefore, inverse filtering works well only if the SNR of the degraded image is high.

One approach to overcoming this difficulty is to preprocess the image by a noise reduction system before performing inverse filtering [7], as shown in Figure 5.1(b). This technique would increase the SNR in order that the deblurring would perform better. One desired property of the noise reduction system

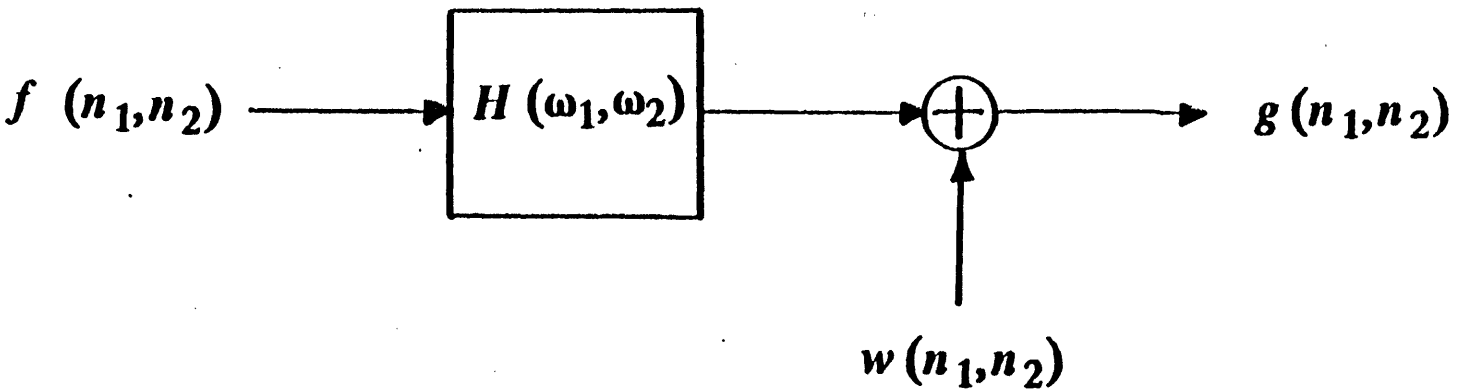

Figure 5.1 (a) Degradation model of images degraded by blurring and additive noise.

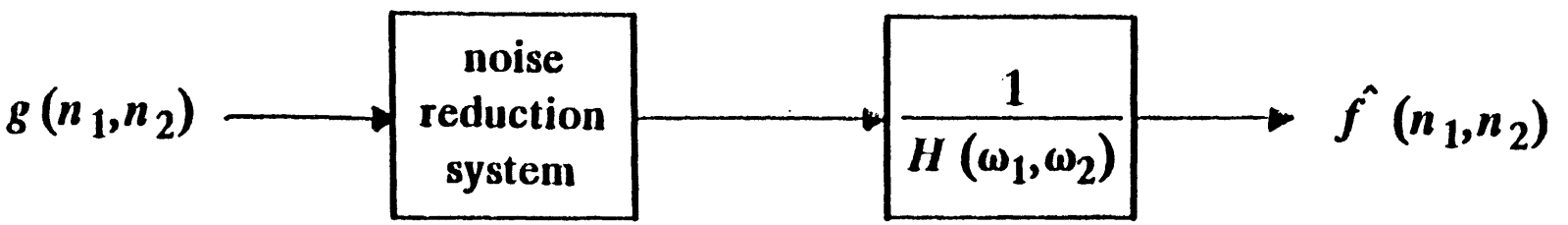

Figure 5.1 (b) A deblurring system using inverse filter.

is that it must have good noise reduction and edge preserving capabilities, in order not to introduce additional blurring to the image. Based on the results presented in the last chapter, the 1-D LLSE algorithm is selected.

5.2.2 Experimental Results

The 'BANK' and 'GIRL' images shown in Figures 4.2 and 4.3 were blurred by a Gaussian shape point-spread function with standard deviation σ equal to 1 pixel. White Gaussian noise was then added to the blurred image. Examples of the degraded images at a blurred-signal to noise ratio (BSNR) of 20 dB are shown in Figure 5.2. Inverse filtering, both with and without the noise reduction system, was carried out. In implementing the inverse filter, it is necessary to set $H(\omega_1,\omega_2)$ to a minimum value if $H(\omega_1,\omega_2)$ falls below a certain level, determined subjectively to give the best visual result. This is to avoid any singularity or near singularity that $H(\omega_1,\omega_2)$ may have. The results of inverse filtering without noise reduction are shown in Figures 5.3(a) and (b). Although inverse filtering sharpens the image, it also introduces additional noise to the image. The results of noise reduction before inverse filtering are shown in Figure 5.3(c) and (d). Much better improvement in image quality can be seen. These results are consistent with those reported in [7].

5.3 Restoration of Images Degraded by Multiplicative Noise

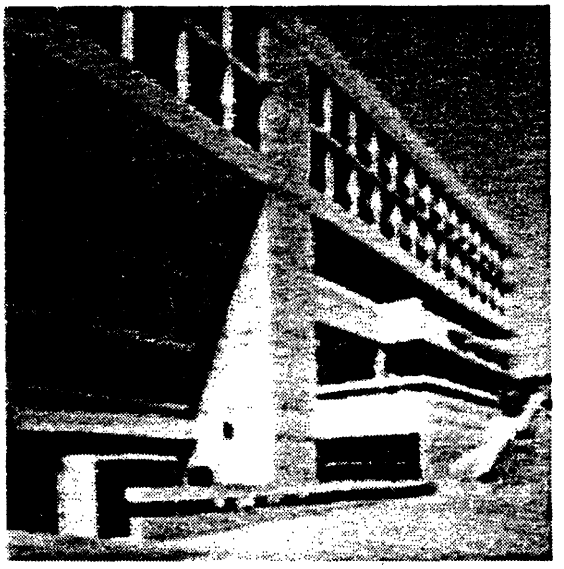

(a)

(b)

Figure 5.2 (a) Figure 4.4(a) blurred by a Gaussian PSF and degraded by additive noise at BSNR = 20dB. (b) Figure 4.5(a) blurred by a Gaussian PSF and degraded by additive noise at BSNR = 20dB.

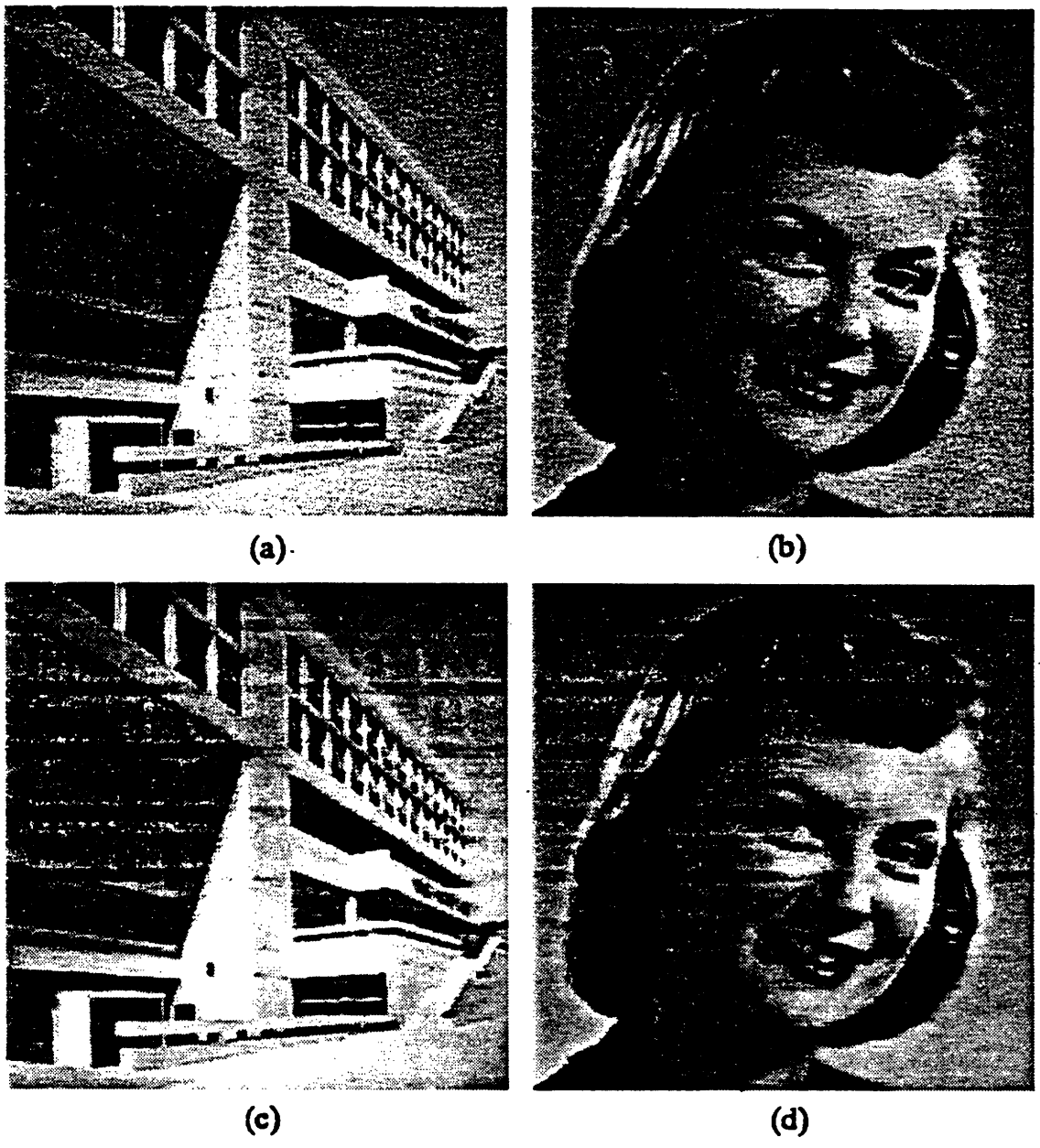

Figure 53 (a) Figure 52(a) restored by inverse filter.
(b) Figure 52(b) restored by inverse filter.
(c) Figure 52(a) restored by noise reduction followed by inverse filter.
(d) Figure 52(b) restored by noise reduction followed by inverse filter.

5.3.1 Filtering of Speckle Degraded Images in the Density Domain

Some physical noise processes are signal-dependent. In many instances, the signal-dependency may be modeled by a multiplicative process. By taking logarithm of the image intensity, one can transform the image into the density domain, and convert the multiplicative noise into an additive one. Thus, filtering techniques, developed for removing additive noise, may be applied in the density domain, and the result converted back into the intensity domain by exponentiation.

One particular example that will be considered here is that of speckle noise in images generated by highly coherent sources, such as laser light. It was shown [8] that speckle noise may be modeled as a signal-independent multiplicative noise. The degraded image can thus be written as

$$g(n_1,n_2) = f(n_1,n_2) \cdot w(n_1,n_2) \tag{5.4}$$

where $w(n_1,n_2)$ is a signal-independent white noise sequence whose probability density function may be modeled by

$$P_{w(n_1,n_2)}(w) = \begin{cases} e^{-w} & w > 0 \\ 0 & \text{otherwise} \end{cases} \tag{5.5}$$

In the density domain, Eqn. (5.4) becomes

$$\log[g(n_1,n_2)] = \log[f(n_1,n_2)] + \log[w(n_1,n_2)] \tag{5.6}$$

Several techniques for reducing speckle noise were studied by Lim and Nawab [8]. The study indicates that if only one frame of the degraded image is available for processing, the results are rather poor due to the very low SNR of the image. However, if N frames of the same image degraded by independent

speckle noise are available, averaging the N frames, followed by a good filtering technique in the density domain, produces much better results. The overall system for restoring speckle noise degraded images by such a scheme is shown in Figure 5.4. In [8], the short space spectral subtraction technique was proposed for the noise reduction system. An alternative that may be used is the 1-D LLSE algorithm. Experimental results of the system using the 1-D LLSE algorithm are shown in the next section.

5.3.2 Experimental Results

The 'BANK' and 'GIRL' images in Figures 4.3 and 4.4 were degraded according to Eqn. (5.4) by a noise sequence whose PDF is given by Eqn. (5.5). Examples of the degraded images are shown in Figures 5.5(a) and (b). Figures 5.5(c) and (d) show the results of averaging eight frames of independently degraded images. These degraded images were restored in the density domain by the 1-D LLSE algorithm. In implementing this algorithm, the variance of $\log[w(n_1,n_2)]$ was taken as $\frac{\pi^2}{6}$ for the single-frame case, and $\frac{1}{N}$ for the N-frame case. The results are shown in Figure 5.6. For the single-frame case, although the speckle noise is significantly reduced, the quality of the image is still poor. For the N-frame case, better noise reduction and preservation of details can be seen.

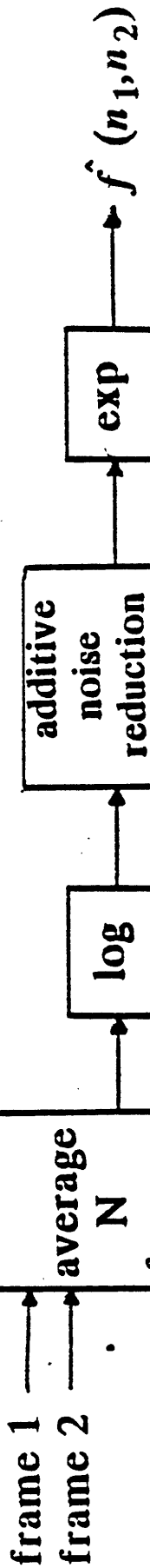

Figure 5.4 **A system for restoring speckle degraded image when N frames of independently degraded images are available.**

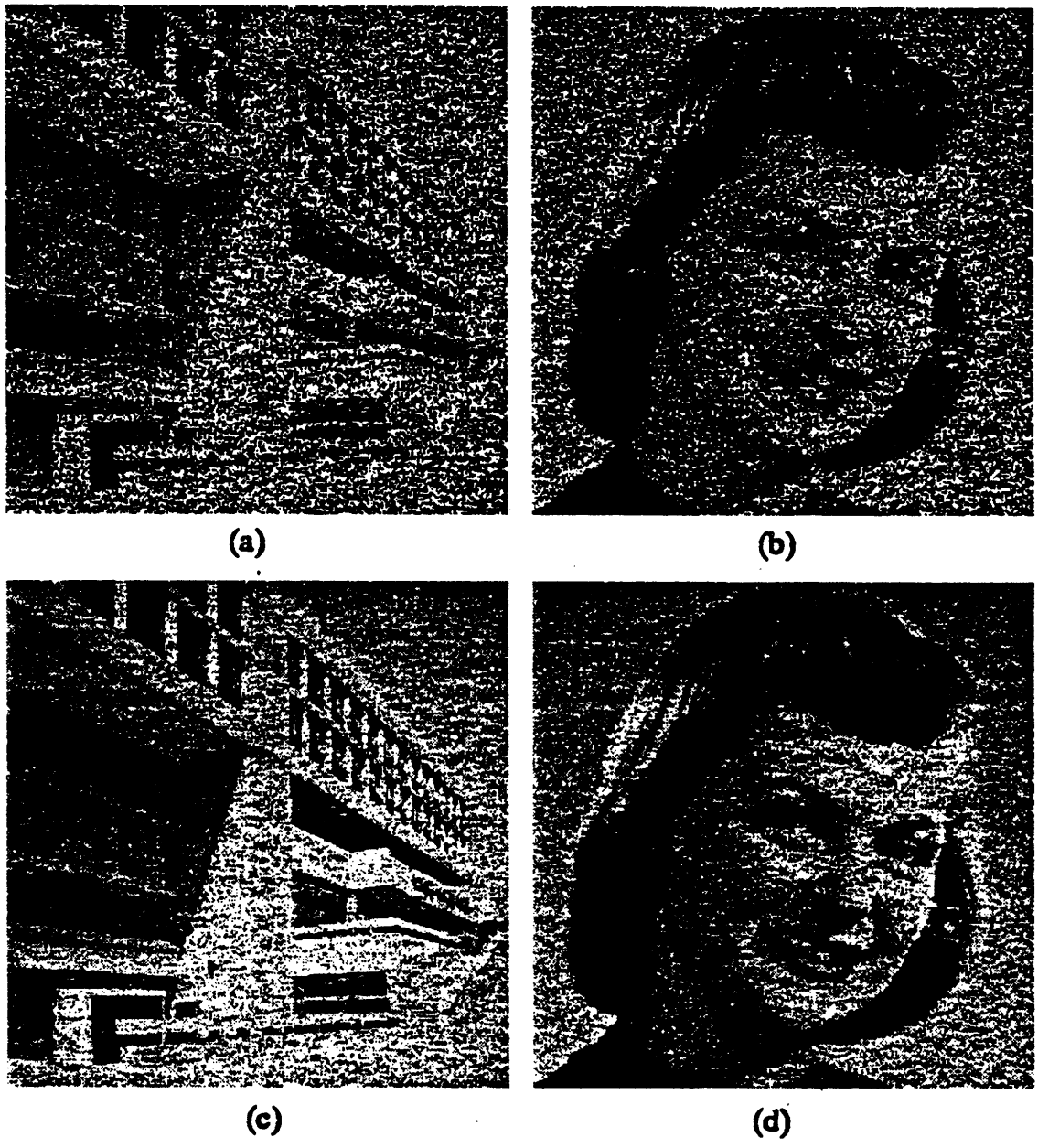

Figure 5.5 (a) Figure 4.4(a) degraded by speckle noise modeled by Eqn. (5.4).

(b) Figure 4.5(a) degraded by speckle noise modeled by Eqn. (5.4).

(c) Result of averaging 8 frames of independently degraded 'BANK' images.

(d) Result of averaging 8 frames of independently degraded 'GIRL' images.

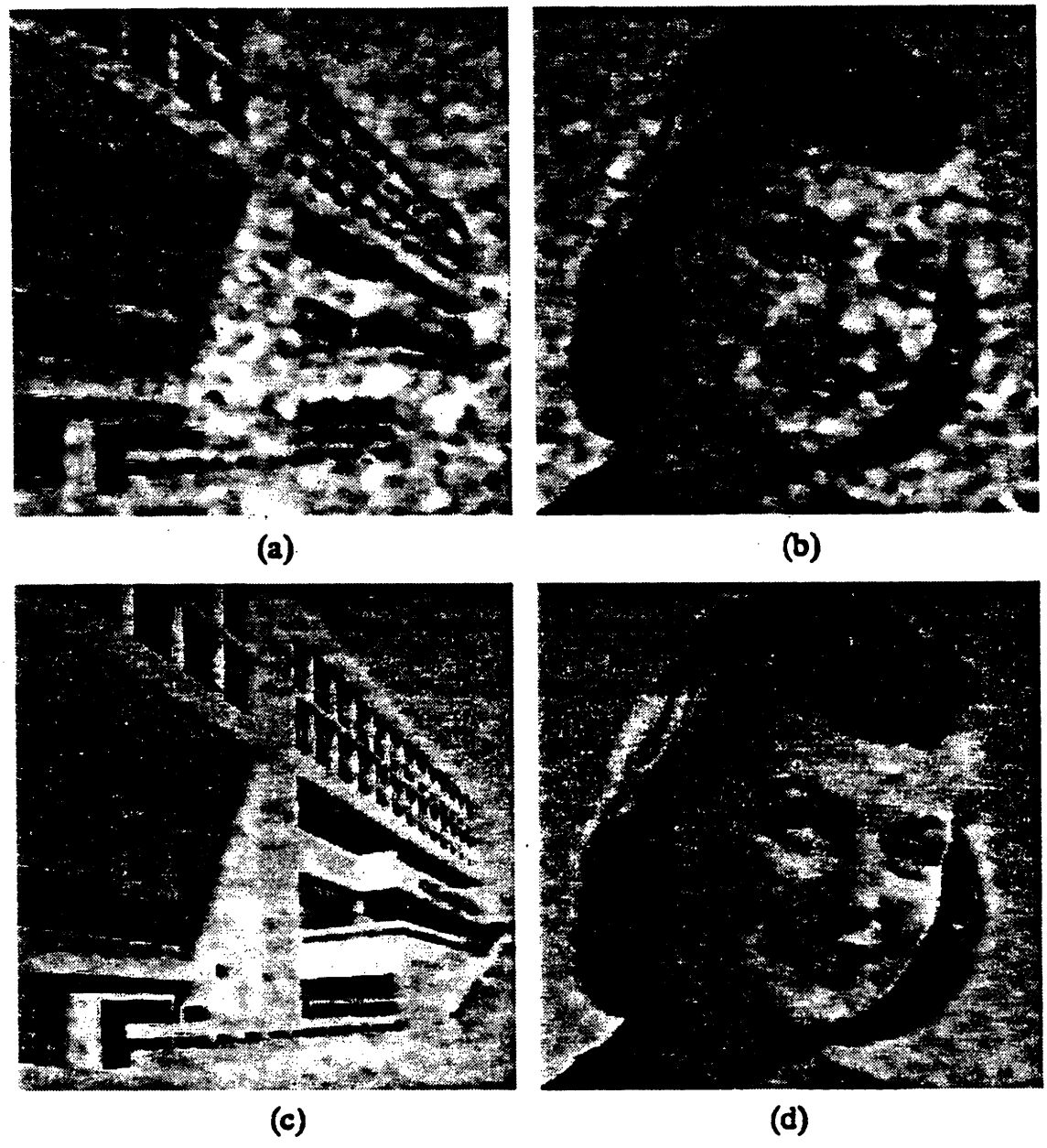

Figure 5.6 Restoration of figure 5.5 by the 1-D LLSE algorithm in the density domain.

(a) Restoration of figure 5.5(a).

(b) Restoration of figure 5.5(b).

(c) Restoration of figure 5.5(c).

(d) Restoration of figure 5.5(d).

5.4 An Application to Noise Reduction in Image Coding

5.4.1 A Quantization Noise Reduction Scheme

One major problem in image coding by pulse code modulation (PCM) techniques is the quantization noise that arises from representing the continuous tone of an image by a finite number of intensity levels. If the number of bits per pixel is reduced to less than 4, the 'staircase' or contouring effect of quantization noise becomes very objectionable. To achieve better image quality in a low bit rate (e.g., 3 bits per pixel) PCM system, Roberts [9] proposed a technique which transforms the contouring effect into a less objectionable signal-independent random noise. In his technique, shown in Figure 5.7(a), a pseudorandom noise sequence is added to the image before quantization. The noise sequence, $w(n_1,n_2)$, is generated by the probability density function given by

$$P_{w(n_1,n_2)}(w) = \begin{cases} \dfrac{1}{\Delta} & |w| \le \dfrac{\Delta}{2} \\ 0 & \text{otherwise} \end{cases} \tag{5.7}$$

where Δ is the quantization level. At the receiver, an exact replica of $w(n_1,n_2)$ is subtracted from the image. Although the noise level in the resulting image is higher, it is more tolerable than the quantization noise.

One way to further improve Roberts' scheme was proposed by Lim [10]. In his system, shown in Figure 5.7(b), a noise reduction system was cascaded to Roberts' system at the receiver to reduce the amount of the added random noise. Significant improvement in image quality was reported. In this

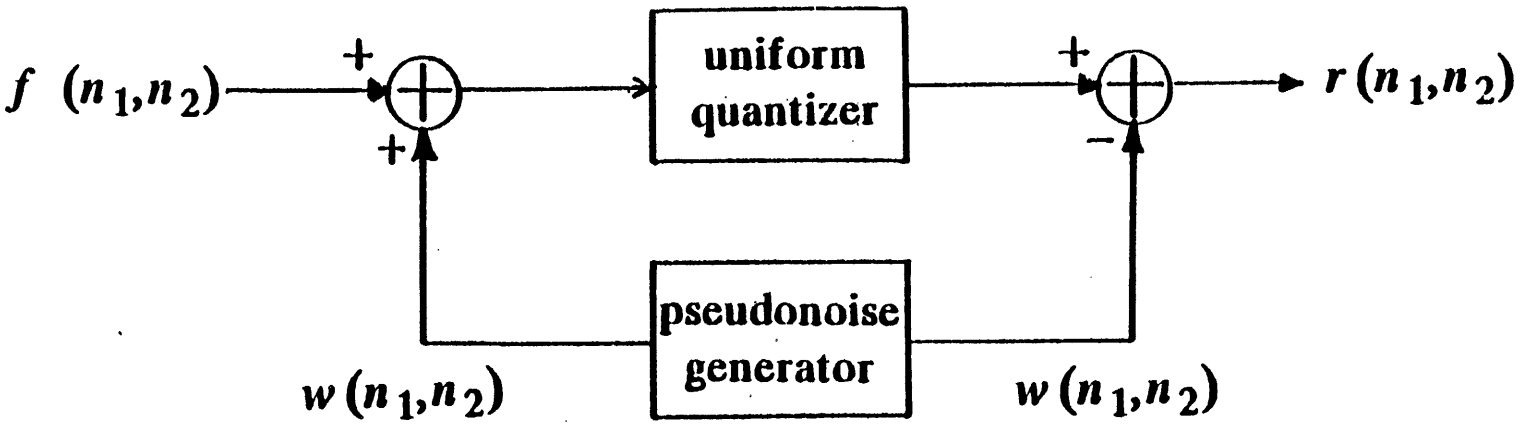

Figure 5.7 (a) Roberts' pseudonoise technique.

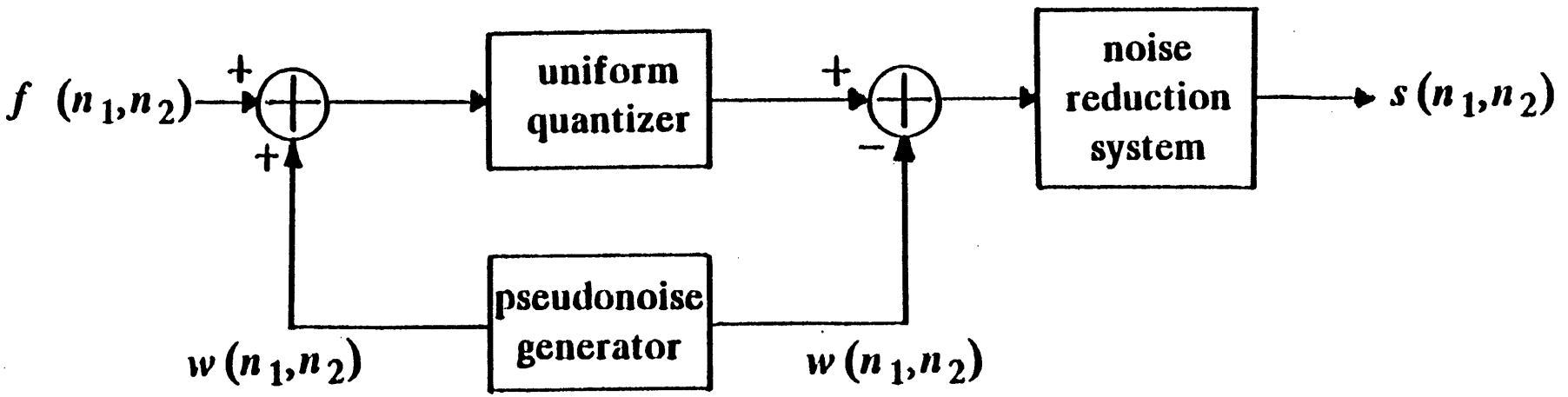

Figure 5.7 (b) An improved technique for quantization noise reduction.

section, the 1-D LLSE algorithm is proposed for the noise reduction system.

5.4.2 Experimental Results

The 'BANK' and 'GIRL' images in Figures 4.3(a) and 4.4(a) were quantized to 3 bits per pixel, as shown in Figures 5.8(a) and 5.9(a). In these pictures, the contouring effect can be seen quite clearly. Roberts' method was implemented, and the results are shown in Figures 5.8(b) and 5.9(b). Although the contouring effect is eliminated, the presence of random noise in the images is quite noticeable. The 1-D LLSE algorithm was then applied to Figures 5.8(b) and 5.9(b). In this algorithm, the noise variance was calculated from Eqn. (5.7) as $\frac{\Delta^2}{12}$. The results, presented in Figures 5.8(c) and 5.9(c), show that much of the random noise is effectively removed while the image resolution is maintained. The experiments were repeated for a 2-bit PCM system. The corresponding images are shown in Figures 5.10 and 5.11.

Table 5.1 lists the the normalized mean-square-error (NMSE) achieved by the two quantization noise reduction schemes in comparison with the standard PCM system. The NMSE (in %) of an image, say, $r(n_1,n_2)$, with respect to the original image $f(n_1,n_2)$, is defined [10] as

$$NMSE = 100 \frac{\sum_{n_1}\sum_{n_2}[r'(n_1,n_2)-f(n_1,n_2)]^2}{\sum_{n_1}\sum_{n_2}[f(n_1,n_2)-m_f]^2} \tag{5.8}$$

where m_f is the mean of $f(n_1,n_2)$, and

$$r'(n_1,n_2) = a \cdot r(n_1,n_2) + b \tag{5.9}$$

(a)

(b)

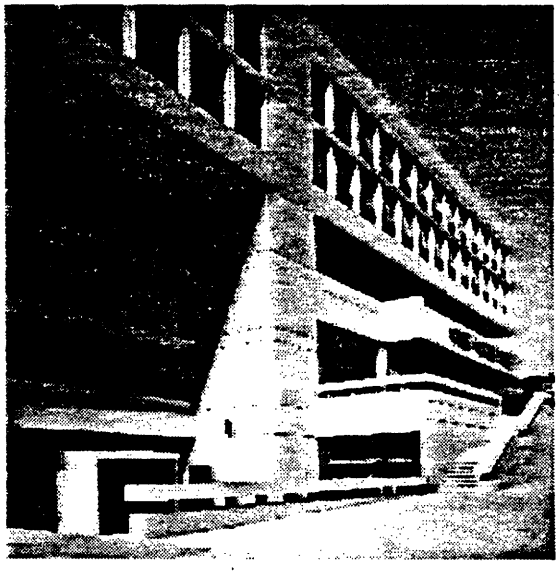

(c)

Figure 5.8 3-bit PCM 'BANK' image.

(a) Standard PCM.

(b) Roberts' pseudonoise technique.

(c) The improved technique.

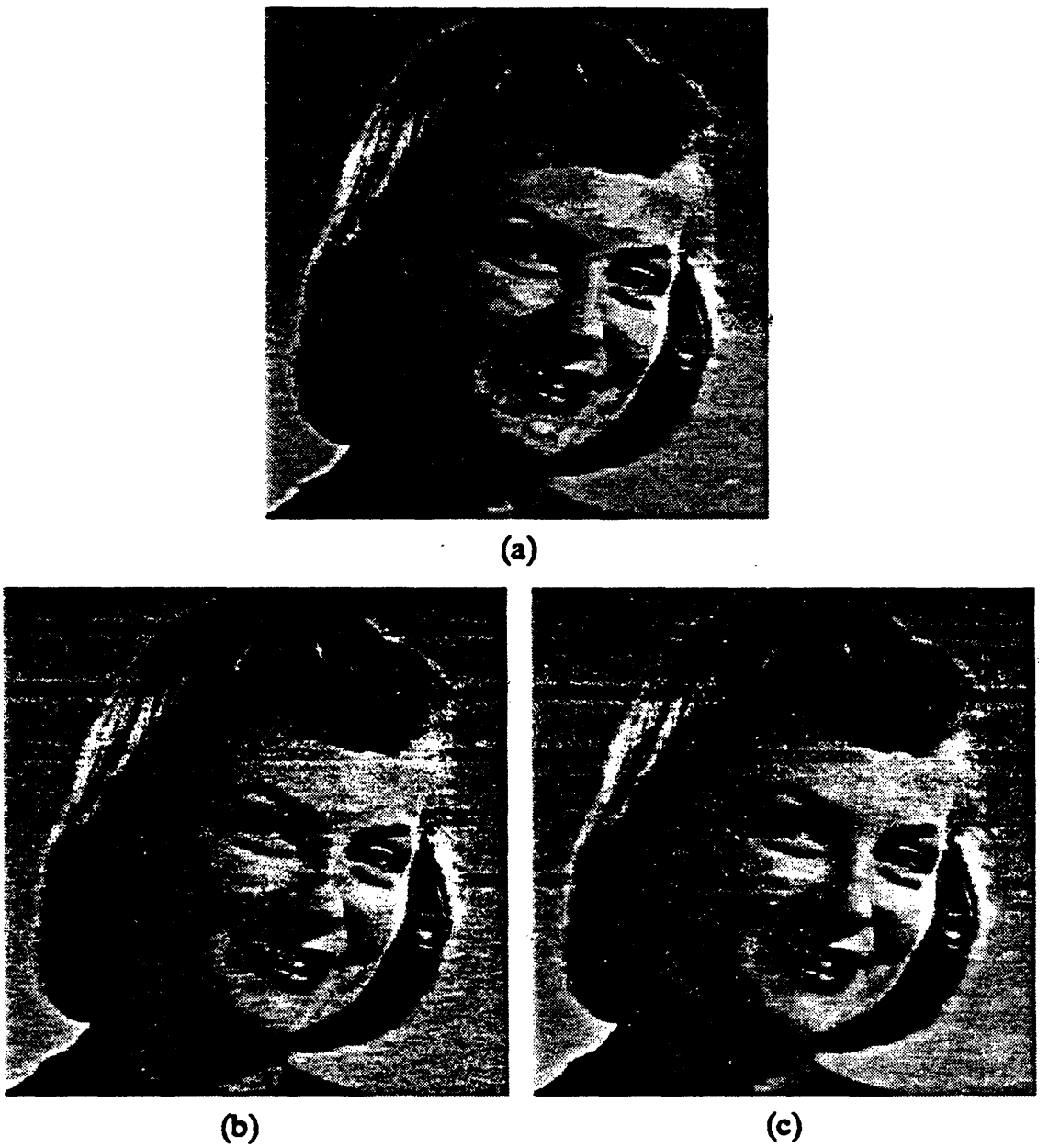

(a)

(b)

(c)

Figure 59 3-bit PCM 'GIRL' image.

(a) Standard PCM.

(b) Roberts' pseudonoise technique.

(c) The improved technique.

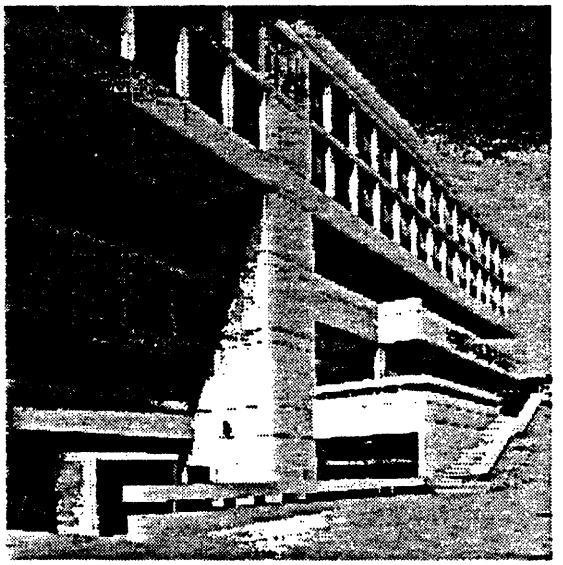

(a)

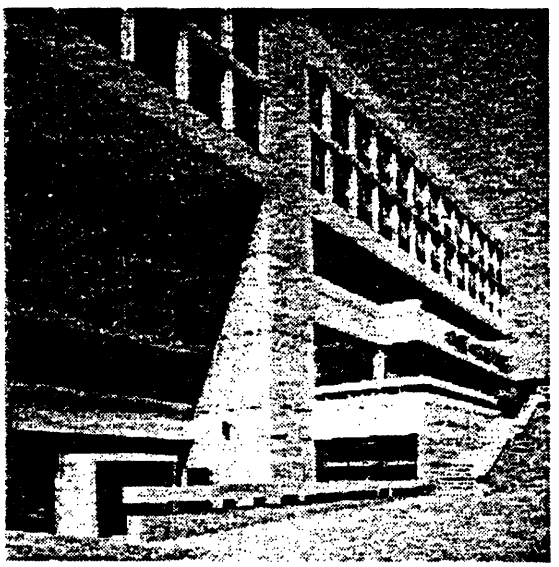

(b)

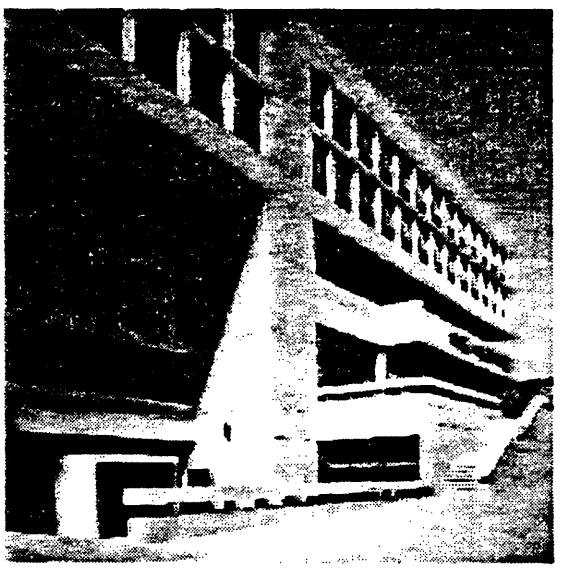

(c)

Figure 5.10 2-bit PCM 'BANK' image.

(a) Standard PCM.

(b) Roberts' pseudonoise technique.

(c) The improved technique.

(a)

(b)

(c)

Figure 5.11 2-bit PCM 'GIRL' image.

(a) Standard PCM.

(b) Roberts' pseudonoise technique.

(c) The improved technique.

with a and b chosen such that $f(n_1,n_2)$ and $r'(n_1,n_2)$ have the same mean and variance. As seen in Table 5.1, the NMSE's of images processed by Roberts' method are significantly lowered by the 1-D LLSE nose reduction algorithm. These results are consistent with the results reported in [10].

Table 5.1: Quantization noise reduction - normalized mean square error (%)

Image	no. of bits per pixel	standard PCM coding	Roberts' pseudonoise method	Roberts' method with 1-D LLSE
BANK	2	8.89	10.61	3.92
BANK	3	2.19	2.50	1.19
GIRL	2	10.83	17.23	4.59
GIRL	3	2.98	3.85	1.56

5.5 Conclusion

Three specific applications of a restoration technique based on the 1-D approach were shown. In each application, the problem was formulated such that a part of the overall restoration system made use of the additive noise reduction scheme. In the first application, the 1-D technique reduced the instability of inverse filter in a deblurring system. In the second application which dealt with multiplicative noise, the 1-D technique was shown to be equally effective in the density domain. In the third application, the 1-D technique improved the Roberts' quantization noise reduction technique by reducing the

amount of the added pseudorandom noise in the image. These results are similar to previous results reported in [7,8,10]. These examples illustrate the usefulness of the 1-D approach for other restoration problems in addition to those involving additive noise, as shown in the last chapter.

CHAPTER 6

SUMMARY AND CONCLUSION

6.1 Summary

In this thesis, a new 1-D approach to adaptive image restoration is presented. The objective of this approach is to improve the performance of the more general 2-D approach for some adaptive image restoration systems which do not model edges adequately. More specifically, techniques based on the new approach remove noise more effectively in the edge as well as non-edge regions, while preserving the resolution of the image.

A brief review of both nonadaptive and adaptive image restoration were presented in Chapter 2, with specific examples to illustrate their general principles. Examples were also presented to show the various ways to approximate the more general 2-D approach by 1-D filters. Such approximations were used partly because of the difficulty in obtaining a good accurate model of the edge, and partly to reduce computations.

Based on the review in Chapter 2, the new 1-D approach was presented in Chapter 3. This approach was motivated by the ability of 1-D filters to smooth noise close to an edge, and the ability of adaptive filters to preserve edges. The general form of restoration techniques based on this approach is shown in Figure 3.1(b), where four 1-D filters are cascaded. Each of the 1-D filters is designed based on the same principle as the more general 2-D adaptive restoration principle, but is oriented respectively in the four major correlation directions of the image, namely, 0, 90, 45, and 135 degrees. The approach was

compared with other 1-D approaches which approximate the 2-D approach.

Examples were presented to demonstrate the effectiveness of the approach. Specifically, the 1-D LLSE algorithm and the 1-D S-type filter, each developed respectively from their 2-D counterparts [5,6], performed better than the 2-D approaches in their ability to reduce noise and maintain resolution. In another example, the 1-D spectral subtraction method did not perform better than the 2-D approach [7], due to the superiority of the latter in modeling edges. However, the 1-D technique reduced the amount of harmonic patterns observed in images restored by the 2-D technique.

Techniques based on the 1-D approach may also be used in conjunction with the inverse filter to restore blurred and noisy images. Results presented in Chapter 5 showed that by performing noise reduction prior to inverse filtering, the ill-conditioning of inverse filtering could be reduced. Transforming an image into the density domain enabled the 1-D technique to be used to restore images degraded by multiplicative noise, such as speckle noise. Since the SNRs of speckle images were typically very low, it was necessary to average several independently degraded images before filtering to obtain better results. In another application, the 1-D technique improved the Roberts' pseudonoise technique for quantization noise reduction. The results obtained in these applications are similar to those obtained using the 2-D short space spectral subtraction technique [7,8,10].

6.2 Suggestions for Future Work

Although the 1-D approach presented in this thesis is based on a simple and somewhat heuristic principle, the results obtained are very encouraging. Several refinements and extensions of the present work are suggested in this section.

In the 1-D algorithms presented in Chapter 4, it was necessary to assume that remaining noise after every 1-D filtering is white, in order to simplify calculation. This was only an approximation, as each filter not only reduced the amount of noise, but also introduced spatial correlation to the noise, and correlation between the image and the noise. In some cases, such as the LLSE algorithm, it is difficult for the algorithm to incorporate colored noise. In others, such as the spectral subtraction technique, colored noise is allowed, and therefore the approximate noise spectrum may be calculated and incorporated into the algorithm. Although this will increase the amount of calculation, it may result in further performance improvement for the 1-D techniques.

The 1-D approach presented is designed for the restoration of an image frame by frame. The same approach may be extended to filtering motion pictures where, in addition to the horizontal and vertical axes, the temporal axis is introduced. In this three-dimensional system, the number of 1-D filters would become 13, instead of 4.

In the examples presented in this thesis, the techniques based on the proposed 1-D approach were designed using the same principle as their 2-D counterparts. There is no reason why the same principles of the existing 2-D

methods have to be used. For example, the LLSE algorithm can be viewed as an example of a two-channel process as shown in Figure 4.1. In this process, the high pass signal is scaled by a particular function of its variance. One modification of the 1-D LLSE algorithm may be to select some other nonlinear functions to further improve the edge preserving capability of the 1-D algorithm.

As a further extension, an entirely new restoration algorithm might be developed based on the general principle of the proposed 1-D approach. The algorithm would then be implemented as four 1-D filters, each not necessarily based on any existing restoration principle. The development of each 1-D filter would be based only on 1-D design techniques, thus avoiding problems that might be encountered in designing 2-D filters.

6.3 Conclusion

Based on the examples shown in this thesis, we conclude that the 1-D approach developed in this thesis can improve the performance of the more general 2-D techniques for some adaptive image restoration systems. Although this is not a general approach that can be applied to the majority of existing image restoration schemes, it has potential to be useful in developing new restoration techniques.

REFERENCES

[1] H. C. Andrews and B. R. Hunt, *Digital Image Restoration*, Englewood Cliffs, NJ, Prentice Hall, 1977.

[2] H. C. Andrews, "Digital Image Restoration: A survey," *Computer*, vol. 8, p36, May, 1975.

[3] N. E. Nahi, "Role of Recursive Estimation in Statistical Image Enhancement," *Proc. IEEE*, vol. 60, p872, July, 1972.

[4] D. P. Panda, "Nonlinear Smoothing of Pictures," *Computer Graphics and Image Processing*, vol. 8, p259, 1978.

[5] J. S. Lee, "Digital image enhancement and noise filtering by use of local statistics," *IEEE Trans. Pattern Analysis and Machine Intelligence*, vol. PAMI-2, No. 2, p165, March, 1980.

[6] G. L. Anderson, A. N. Netravali, "Image restoration based on a subjective criterion," *IEEE Trans. Systems, Man and Cybernetics*, vol. SMC-6, No. 12, p845, Dec 1976.

[7] J. S. Lim, "Image restoration by short space spectral subtraction," *IEEE Trans. Acoustic, Speech and Signal Processing*, vol. ASSP-28, No2, p191, April 1980.

[8] Jae S. Lim and H. Nawab, "Techniques for Speckle Noise Removal," *Optical Engineering*, vol. 20, No. 3, p472, May, 1981.

[9] L. G. Roberts, "Picture Coding Using Pseudonoise", *IRE Trans. Information Theory*, vol. IT-8, p145, 1962.

[10] Jae S. Lim, "Reduction of Quantization Noise in Pulse Modulation Image Coding", *Optical Engineering*, vol. 19, No. 4, p577, July, 1980.

[11] C. W. Helstrom, "Image Restoration by the Method of Least Squares", *J. Opt. Soc. Am.*, 57, p297, 1967.

[12] A. Habibi, "Two-dimensional Bayesian Estimate of Images," *Proc. IEEE*, vol. 60, p878, July, 1972.

[13] H. J. Trussell and B. R. Hunt, "Sectioned methods for image restoration," *IEEE Trans. Acoustic, Speech and Signal Processing*, vol. ASSP-26, No2, p157, April 1978.

[14] S. A. Rajala and R. J. P. de Figueiredo, "Adaptive nonlinear image restoration by a modified Kalman filtering approach," *IEEE Trans. Acoustic, Speech and Signal Processing*, vol. ASSP-29, No. 5, p1033, Oct, 1981.

[15] D. S. Lebedev and L. I. Mirkin, "Smoothing of two-dimensional images using the 'composite' model of a fragment," *Iconics-Digital Holography-Image Processing*, Institute for Problems in Information Transmission, Academy of Sciences, USSR, p57, 1975.

[16] J. F. Abramatic and L. M. Silverman, "Nonlinear restoration of noisy images," *IEEE Trans. Pattern Analysis and Machine Intelligence*, vol. PAMI-4, No2, p141, March, 1982.

[17] A. C. Bovik, T. S. Huang and D. C. Munson Jr., "Image restoration using order constrained least-squares methods," *Proc. IEEE ICASSP 83*, Boston, MA, p828, April, 1983.

[18] B. R. Hunt and T. M. Cannon, "Nonstationary assumptions for Gaussian models of images," *IEEE Trans. Systems, Man and Cybernetics*, vol. SMC-6, No. 12, p878, Dec, 1976.

[19] H. Nawab, A. V. Oppenheim and J. S. Lim, "Improved Spectral Subtraction for Signal Restoration", *Proc. IEEE ICASSP 81*, p1105, March, 1981.

DISTRIBUTION LIST

	DODAAD Code	
Director Advanced Research Project Agency 1400 Wilson Boulevard Arlington, Virginia 22209 Attn: Program Management	HX1241	(1)
Group Leader Information Sciences Associate Director for Engineering Sciences Office of Naval Research 800 North Quincy Street Arlington, Virginia 22217	N00014	(1)
Administrative Contracting Officer E19-628 Massachusetts Institute of Technology Cambridge, Massachusetts 02139	N66017	(1)
Director Naval Research Laboratory Attn: Code 2627 Washington, D.C. 20375	N00173	(6)
Defense Technical Information Center Bldg. 5, Cameron Station Alexandria, Virginia 22314	S47031	(12)